nature cell biology

A kinase cascade leading to Rab11-FIP5 controls transcytosis of the polymeric immunoglobulin receptor

Tao Su[1,2], David M. Bryant[1,2,9], Frédéric Luton[1,2,3,9], Marcel Vergés[1,2,4], Scott M. Ulrich[5,6], Kirk C. Hansen[7,8], Anirban Datta[1,2], Dennis J. Eastburn[1,2], Alma L. Burlingame[7], Kevan M. Shokat[5] and Keith E. Mostov[1,2,10]

Polymeric immunoglobulin A (pIgA) transcytosis, mediated by the polymeric immunoglobulin receptor (pIgR), is a central component of mucosal immunity and a model for regulation of polarized epithelial membrane traffic. Binding of pIgA to pIgR stimulates transcytosis in a process requiring Yes, a Src family tyrosine kinase (SFK). We show that Yes directly phosphorylates EGF receptor (EGFR) on liver endosomes. Injection of pIgA into rats induced EGFR phosphorylation. Similarly, in MDCK cells, pIgA treatment significantly increased phosphorylation of EGFR on various sites, subsequently activating extracellular signal-regulated protein kinase (ERK). Furthermore, we find that the Rab11 effector Rab11-FIP5 is a substrate of ERK. Knocking down Yes or Rab11-FIP5, or inhibition of the Yes–EGFR–ERK cascade, decreased pIgA–pIgR transcytosis. Finally, we demonstrate that Rab11-FIP5 phosphorylation by ERK controls Rab11a endosome distribution and pIgA–pIgR transcytosis. Our results reveal a novel Yes–EGFR–ERK–FIP5 signalling network for regulation of pIgA–pIgR transcytosis.

Membrane traffic must be tightly, yet flexibly, regulated to control the composition of cellular compartments under changing physiological and developmental conditions[1–4]. In epithelial cells, the transcytosis of pIgA by the pIgR is used as a model to study such regulation. Transcytosis of the pIgA–pIgR complex from the basolateral plasma membrane to the apical plasma membrane occurs in mucosal epithelia during immune defence[5]. The pIgR is targeted from the trans Golgi network (TGN) to the basolateral plasma membrane where it can bind pIgA, is endocytosed into endosomes and then transcytosed to the apical plasma membrane. Although pIgR is transcytosed in the absence of pIgA, binding of pIgA increases the efficiency and rate of transcytosis[6,7] through initiation of a signal-transduction pathway; this is a paradigm for how the binding of cargo to a receptor can autoregulate traffic[8]. The regulation of pIgA transcytosis is also central for the understanding of mucosal immunity[9]. IgA-secreting plasma cells can produce more pIgA in response to infection and the ability of this increased pIgA to stimulate its own transcytosis enables coordination of transcytosis with other aspects of mucosal immunity. Furthermore, transcytosis is a universal mechanism for delivery of proteins to the apical surface of polarized epithelial cells. Therefore, understanding the regulation of the best-understood transcytotic pathway is of general importance[10].

The binding of pIgA primarily stimulates pIgA–pIgR movement from apical recycling endosomes (AREs) to the apical plasma membrane, the last step in transcytosis[11]. Several small GTPases, Rab3b, Rab25, and Rab11a with its effector Rab11-FIP5 (also known as Rip11/pp75; throughout this paper referred to as FIP5), are enriched in the ARE and are involved in polarized protein recycling, and pIgA transcytosis[12–14].

Injection of pIgA into rats activates the Src family tyrosine kinase Yes, and pIgA-stimulated transcytosis is defective in Yes-knockout mice[15]. Thus, pIgA binding triggers signalling that promotes apical delivery of pIgA–pIgR through Yes activation *in vivo*. Identification of Yes substrates is central to understanding the regulation of pIgA transcytosis. Here, we identify a Yes substrate that, when phosphorylated, leads to activation of a kinase cascade that controls pIgA transcytosis.

RESULTS

EGFR is a direct substrate of Yes in rat liver endosomes

To identify substrates of Yes involved in transcytosis, we used a Yes mutant (T346G) fused to a GST tag (denoted as Yes-GTM) in *in vitro* kinase assays. Yes-GTM is myristoylated for membrane targeting, and is engineered to uniquely use only specific ATP analogues, which allowed us to detect direct substrates of Yes-GTM[16,17]. A rat liver endosome fraction enriched in pIgR and Yes was used as the substrate source (receptor recycling compartment;

[1]Department of Anatomy, University of California, San Francisco, CA 94158-2517, USA. [2]Biochemistry and Biophysics, University of California, San Francisco, CA 94158-2517, USA. [3]Institut de Pharmacologie Moléculaire et Cellulaire, Université de Nice Sophia-Antipolis, CNRS-UMR6097, 06560 Sophia-Antipolis, France. [4]Cardiovascular Genetics Centre, IdIBGi - University of Girona, 17003 Girona, Spain. [5]Department of Cellular and Molecular Pharmacology, University of California, San Francisco, CA 94158-2280, USA. [6]Department of Chemistry, Ithaca College, Ithaca, NY 14850, USA. [7]Department of Pharmaceutical Chemistry, University of California, San Francisco, CA 94158-2517, USA. [8]Proteomics Core, University of Colorado Health Sciences Centre, Aurora, CO 80045, USA. [9]These authors contributed equally to this work.
[10]Correspondence should be addressed to K.E.M. (keith.mostov@ucsf.edu).

Received 20 January 2010; accepted 06 October 2010; published online 31 October 2010; corrected online 12 November 2010; DOI: 10.1038/ncb2118

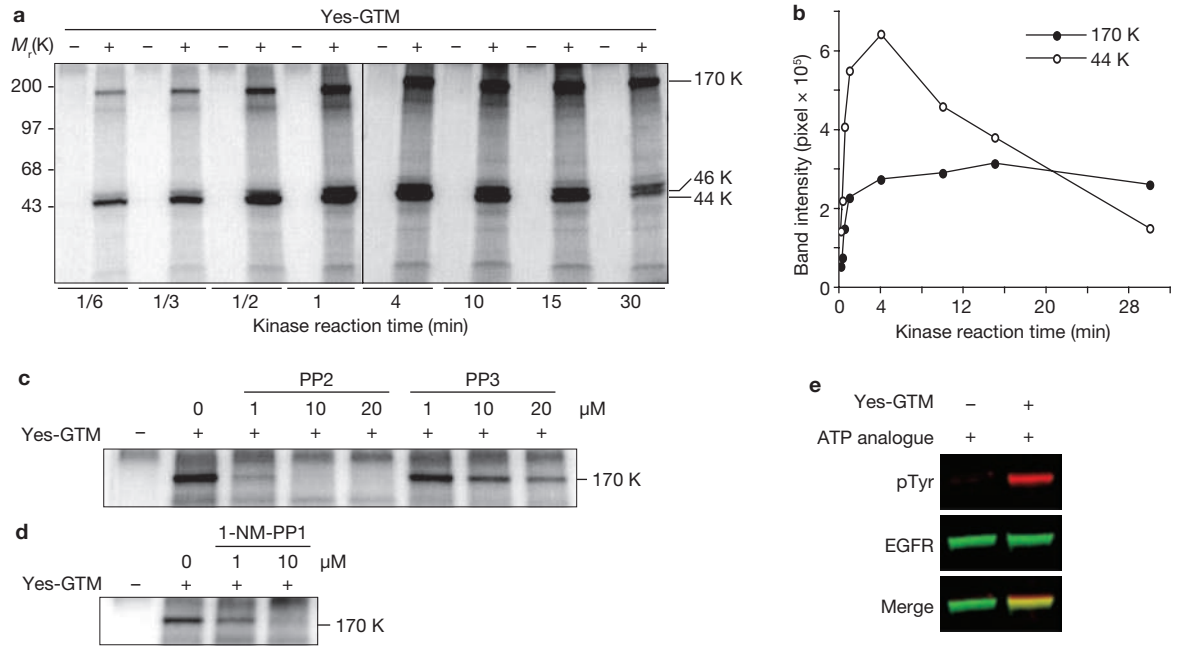

Figure 1 Identification of EGFR as a Yes substrate in rat liver endosomes. (**a**) A Yes-GTM kinase reaction assay was performed *in vitro* on endosomal membranes for the indicated times. Each reaction mixture contained rat liver endosomes and [γ-^{32}P]–N^6(benzyl) ATP, with or without Yes-GTM as indicated. Proteins were separated by SDS–PAGE and ^{32}P-labelled proteins were detected by a phosphorimager. Three major proteins of 170, 46 and 44 K are phosphorylated by Yes-GTM. Boxes indicate separate gels. (**b**) Quantification of the band intensities in **a**. (**c**, **d**) Kinase reaction assays were performed with or without Yes-GTM, and with PP2 or PP3 (**c**) or 1-NM-PP1 (**d**) at the indicated concentrations. Reaction mixtures contained rat liver endosomes and [γ-^{32}P]–N^6(benzyl) ATP. Proteins were separated by SDS–PAGE and ^{32}P-labelled proteins were detected by a phosphorimager. PP3 is an inactive analogue of PP2. (**e**) Protein from endosomes was resolved by SDS–PAGE. Total (green) and phosphorylated EGFR (red) were identified by dual-colour infrared immunoblotting using antibodies specific to EGFR and phosphorylated tyrosine (pTyr). The phosphorylated tyrosine band occurs only in the presence of Yes-GTM, precisely co-migrating with EGFR. Uncropped images of blots are shown in Supplementary Information, Fig. S7.

RRC)[5,18]. To label only Yes-GTM substrates, endosomes were incubated with Yes-GTM and radiolabelled ATP analogue [γ-^{32}P]N^6–(benzyl) ATP. Proteins of 170, 46 and 44 K were phosphorylated, reaching maximum levels of phosphorylation at 4 min (Fig. 1a, b). These proteins were absent in controls lacking Yes-GTM. The general (PP2) or Yes-GTM-specific (1-NM-PP1; ref. 19) SFK inhibitors abolished phosphorylation (170 K band shown; Fig. 1c, d). PP3, an inactive analogue of PP2, demonstrated inhibition only at high concentration (Fig. 1c).

We isolated the 170 K protein using antibodies against phosphorylated tyrosine (Supplementary Information, Fig. S1). By mass spectrometry, it was identified as rat EGFR; seventeen peptides covered approximately 12% of the EGFR. We could not identify the 44 and 46 K species (Fig. 1a) because of co-migrating antibody heavy chain (Supplementary Information, Fig. S1). Simultaneous dual-colour immunoblotting confirmed that the 170 K phosphorylated tyrosine band precisely co-migrates with EGFR (Fig. 1e).

Phosphorylation of EGFR in response to pIgA requires Yes

We confirmed that EGFR is phosphorylated *in vivo* in response to pIgA by injecting rats with pIgA, which binds to pIgR on hepatocytes[20]. After 1 min, we isolated endosomes[15] and detected total and phosphorylated EGFR by immunoprecipitation, followed by immunoblotting with anti-phosphorylated-tyrosine antibody. A 126.4 ± 26.2% increase in the ratio of phosphorylated tyrosine to total EGFR was observed in the RRC of pIgA-injected rats, compared with controls (Fig. 2a, $n = 3$, $P < 0.03$). Thus, pIgA induces stimulation of EGFR phosphorylation *in vivo*.

Next, we studied stimulation of pIgA in MDCK cells expressing rabbit pIgR, which have been used similarly in previous studies. Immunoblots of lysates from pIgR-expressing MDCK cells treated with pIgA had a 170 K phosphorylated tyrosine band, which peaked at 1–5 min after pIgA treatment (Fig. 2b, control). This band precisely co-migrated with the higher-molecular-weight EGFR band (as determined by dual-colour immunoblotting), and therefore represents EGFR with a phosphorylated tyrosine. Quantification of band intensity indicated that the ratio of phosphorylated tyrosine to total EGFR increased to 85 ± 26% at 5 min after the pIgA treatment, compared with cells at 0 min after pIgA treatment ($n = 4$, $P < 0.01$). We expressed *Yes* shRNA in pIgR-expressing MDCK cells, achieving approximately 90% protein reduction. Immunoblotting indicated that the higher-molecular-weight phosphorylated-tyrosine EGFR band induced by pIgA binding was abolished by Yes knockdown (Fig. 2b), or treatment with PP2 (Fig. 2c). No increase in EGFR phosphorylation was detected when parental MDCK cells (no pIgR) were treated with pIgA (data not shown). Thus, pIgA induces Yes-dependent phosphorylation of EGFR in MDCK cells expressing pIgR.

Next, we examined which EGFR tyrosine residues become phosphorylated in response to pIgA treatment using pIgR-expressing MDCK cells that also express human EGFR (hEGFR). On 5 min treatment with pIgA, EGFR phosphorylation increased significantly on Tyr 992 (71 ± 31%), with moderate increases on Tyr 1173 (36 ± 19%) and Tyr 845 (34 ± 11%) ($n = 4$, $P < 0.03$; Fig. 2d). No significant increase was detected at Tyr 1068, Tyr 1086 or Tyr 1045. Thus, EGFR is a substrate of Yes *in vitro* and *in vivo* in a pathway stimulated by pIgA.

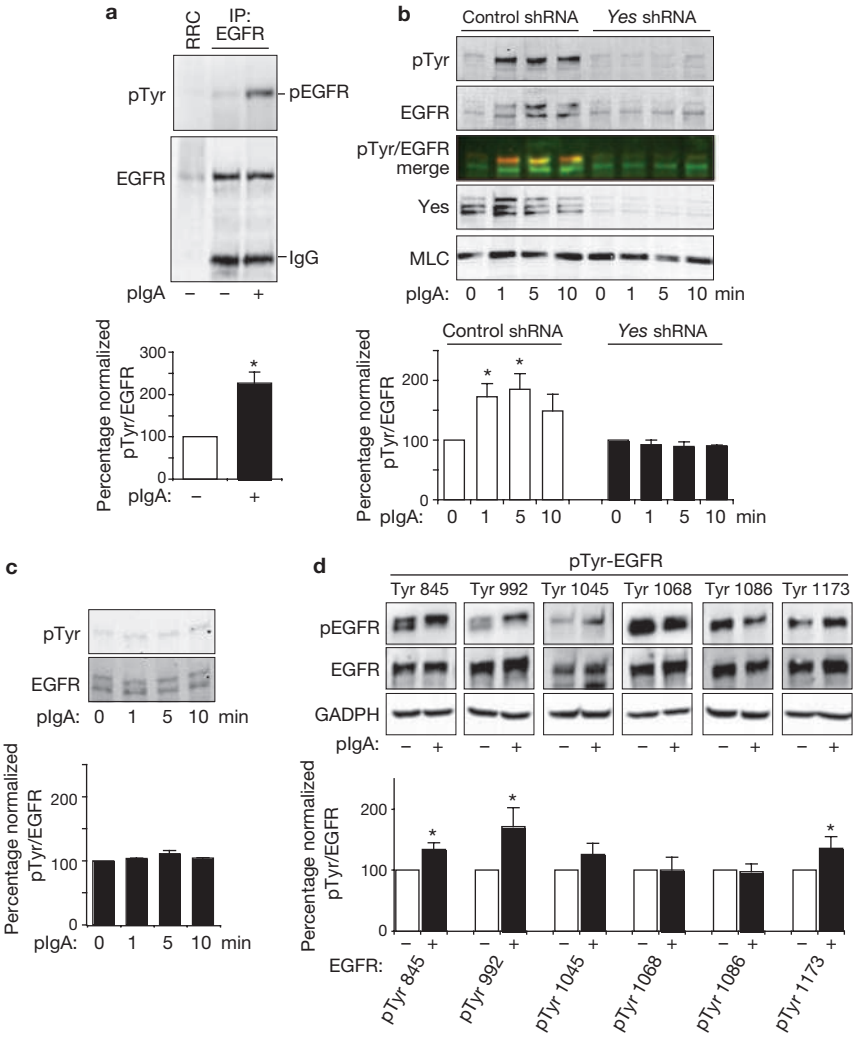

Figure 2 EGFR phosphorylation is induced in rat liver endosomes, and in pIgR-expressing MDCK cells, on pIgA stimulation. (**a**) EGFR phosphorylation in rats injected with pIgA. Top: endosome fractions, from rats treated with pIgA as indicated, were analysed by immunoprecipitation of EGFR, and immunoblotting with antibodies against phosphorylated tyrosine and EGFR. Antibody heavy chains from immunoprecipitation are indicated at the bottom of the blot. IP; immunoprecipitation, pEGFR; phosphorylated EGFR. Bottom: intensity of the phosphorylated tyrosine bands (normalized to EGFR bands), with or without pIgA treatment. Data are means ± s.e.m. Asterisk indicates $P < 0.03$, $n = 3$. (**b**) Top: MDCK cells expressing pIgR and stably expressing control, scrambled-sequence shRNA or *Yes* shRNA were treated basolaterally with pIgA for the indicated times. Cells were lysed and proteins were resolved by SDS–PAGE and immunoblotting with antibodies against phosphorylated tyrosine, EGFR and Yes at the indicated times after pIgA treatment (0 min represents control without pIgA treatment). Colour image represents overlay of phosphorylated tyrosine/EGFR signals from infrared immunoblots. Note precise co-migration of phosphorylated tyrosine and the upper EGFR band in dual-colour immunoblots, representing phosphorylated tyrosine–EGFR. MLC; myosin light chain, loading control. Bottom: intensity of the phosphorylated EGFR bands (normalized to EGFR bands) at indicated times after pIgA treatment. Data are means ± s.e.m. Asterisks indicate $P < 0.01$, compared with control cells at 0 min, $n = 4$. (**c**) Top: pIgR-expressing MDCK cells were treated basolaterally with pIgA for the indicated times in the presence of SFK inhibitor (PP2). Cells were lysed at the indicated times after pIgA treatment and proteins were resolved by SDS–PAGE and immunoblotting. Bottom: intensity of the phosphorylated EGFR bands (normalized to EGFR bands), at indicated times after pIgA treatment. Data are means ± s.e.m., $n = 4$. (**d**) Top: MDCK cells stably expressing hEGFR and pIgR were treated basolaterally with pIgA for 5 min, as indicated. Lysates were immunoblotted with antibodies specific to EGFR proteins phosphorylated at the tyrosine residues indicated at the top, and antibodies against total EGFR and GAPDH (glyceraldehyde-3-phosphate dehydrogenase, as a control). Bottom: intensity of the phosphorylated EGFR bands (phosphorylated at the indicated residues and normalized to EGFR bands), with or without pIgA treatment. Data are means ± s.e.m. Asterisk indicates $P < 0.03$, compared with the respective cells not treated with pIgA ($n = 4$). Uncropped images of blot are shown in Supplementary Information, Fig. S7.

Formation of a pIgR–Yes–EGFR complex at basal state in endosomes

In a previous study, Yes and pIgR were shown to co-immunoprecipitate[15], so we tested if EGFR also co-immunoprecipitates with these proteins. We detected specific co-immunoprecipitation of pIgR, Yes and EGFR from solubilized liver endosomes, compared with no co-immunoprecipitation from non-specific serum (NSS; Fig. 3a). pIgR, Yes and EGFR could also be co-immunoprecipitated from the lysate of MDCK cells expressing hEGFR and pIgR (Fig. 3b). Co-immunoprecipitation efficiencies were approximately 10% (7–13.9%) (Fig. 3a, b). This indicates the existence of a complex, or complexes, between pIgR, Yes and EGFR in MDCK cells, and in endosomes *in vivo*.

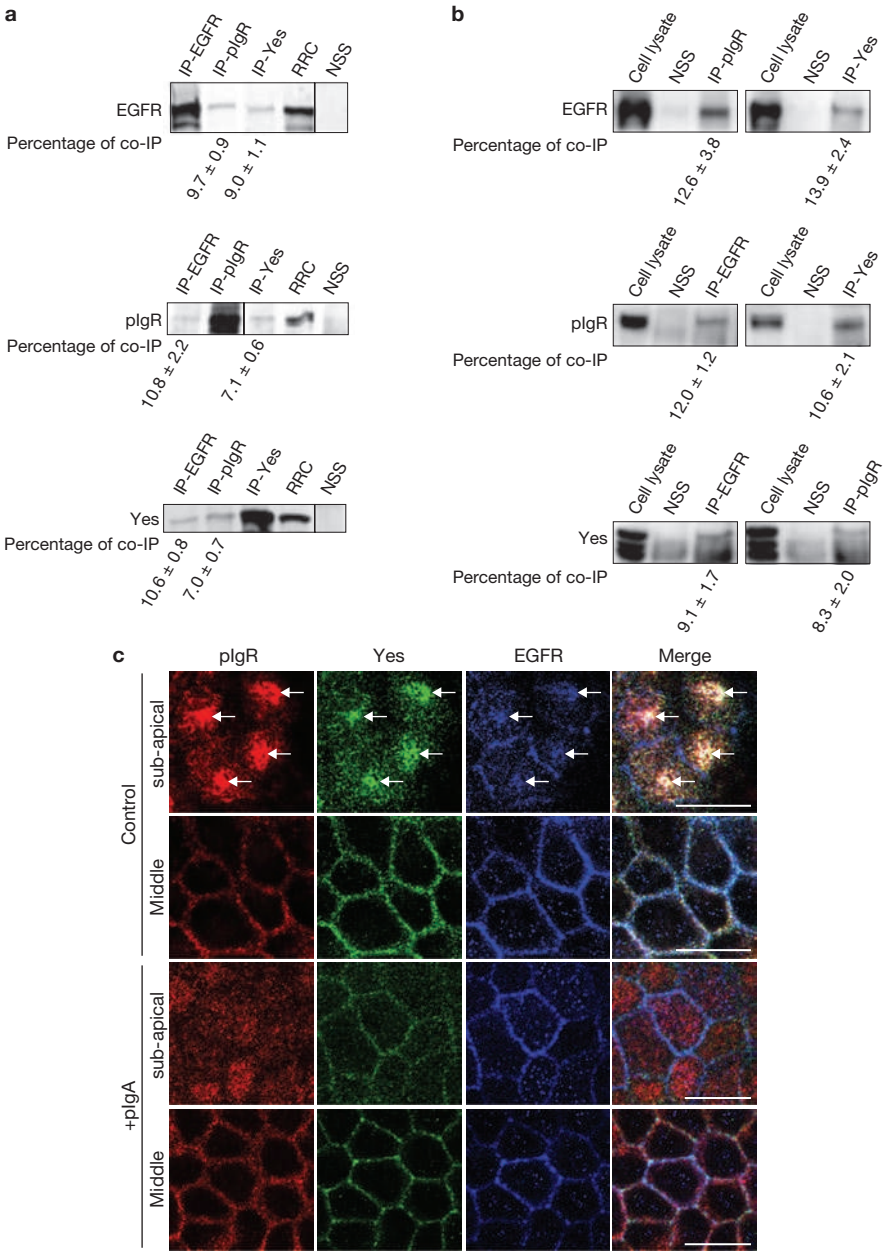

Figure 3 Interaction and co-localization of EGFR, pIgR and Yes. (**a**) Rat liver endosomes were solubilized and EGFR, pIgR or Yes were immunoprecipitated. The proteins were resolved by SDS–PAGE and co-immunoprecipitation was assessed by immunoblotting. Immunoprecipitations with non-specific rabbit serum (NSS) were performed as a negative control. In the RRC lane, 5 μg of protein was loaded as the input. The intensity of the co-immunoprecipitated protein bands are indicated, compared with the intensity of the immunoprecipitated protein bands (data are means ± s.e.m., $n = 4$). Boxes represent spliced regions from same gels, to maintain sample order format under all conditions. (**b**) pIgR, Yes or EGFR were immunoprecipitated from the lysates of MDCK cells expressing hEGFR and pIgR, and co-immunoprecipitation was detected by immunoblotting, as indicated. Immunoblotting of total cell lysates and immunoprecipitation and immunoblotting of non-specific serum (NSS) and was also performed. The intensity of the co-immunoprecipitated protein bands are indicated as a percentage of the intensity of the protein bands in the input lysate (data are means ± s.e.m., $n = 3$). (**c**) Monolayers of MDCK cells expressing hEGFR and pIgR were fixed and stained with antibodies against the indicated proteins for immunofluorescence microscopy. Top: Representative images from the sub-apical and lateral (middle) regions of MDCK cell monolayers. Arrows indicate vesicular co-localization of pIgR, Yes and EGFR. White spots in the merged image indicate intracellular co-localization of EGFR, pIgR and Yes. Bottom: representative images from the sub-apical and lateral (middle) regions of MDCK cell monolayers on pIgA treatment. Scale bars, 20 μm. Uncropped images of blots are shown in Supplementary Information, Fig. S7.

We examined the possible location of pIgR, EGFR and Yes interaction in MDCK cells (Fig. 3c). Partial co-localization of EGFR, pIgR and Yes in vesicles was most apparent in the sub-apical region (Fig. 3c, control cells)[21], although some partial co-localization was observed near cell–cell contacts (Fig. 3, control cells; middle). On addition of pIgA, pIgR labelling dispersed from this sub-apical pool (Fig. 3c, bottom), representing apical transcytosis of pIgR. Dispersed pIgR vesicles were also seen laterally (Fig. 3c, bottom). Quantification revealed partial co-localization of pIgR,

Yes and EGFR primarily in the sub-apical region of cells (Supplementary Information, Fig. S2a). Co-immunoprecipitation of this complex was similarly reduced on pIgA treatment (Supplementary Information, Fig. S2b, c). Co-staining for the ARE-marker Rab11a revealed overlap with a pool of pIgR, but not EGFR, either with or without pIgA stimulation (Supplementary Information, Fig. S2d, e). These data suggest that pIgR, Yes and EGFR form a complex in the sub-apical region before entry into the Rab11a-positive ARE, and that pIgA induces release of pIgR from the complex, probably to allow apical delivery.

Transcytosis of pIgA requires EGFR

To test if pIgA–pIgR transcytosis requires EGFR, we measured apical release of metabolically labelled secretory component, the extracellular fragment of pIgR cleaved at the apical surface on pIgA binding in MDCK cells expressing pIgR. When compared with control cells, addition of pIgA to the basolateral surface of pIgR-expressing MDCK cells stimulated apical-secretory-component release (1.5-fold–2-fold) at 30 and 60 min, as previously shown[6] (Fig. 4a). This was largely blocked by addition of an EGFR inhibitor (PD153035). Similarly, EGFR knockdown decreased apical transcytosis of pIgA (Supplementary Information, Fig. S3a, f), without affecting monolayer polarization or transepithelial resistance (TER) (Supplementary Information, Fig. S3c, d). We hypothesized that stimulation of EGFR with EGF might bypass the need for pIgA to stimulate pIgR transcytosis. Accordingly, addition of EGF caused an early and marked increase in release of apical secretory component (2.5-fold, compared with control cells, at 15 min and equal to pIgA-stimulated transcytosis at 30 min), but declined to baseline levels by 60 min (Fig. 4a). This effect was blocked by pre-treatment with the EGFR inhibitor PD153035. Transcytosis of fluid-phase horse radish peroxidase (HRP) was not affected by pIgA or EGF, suggesting that there was not a general stimulation of transcytosis (Supplementary Information, Fig. S4).

Next, transport of the pIgA ligand was directly measured. We added biotinylated pIgA to the basolateral surface of MDCK cells and measured its apical release and intracellular retention. Overexpression of hEGFR caused a 3-fold increase in apical release at 15 min (Fig. 4b) that declined by 60 min, similarly to the effect of EGF stimulation on apical-secretory-component release (Fig. 4a). In contrast, Yes knockdown decreased pIgA transcytosis significantly at all times, especially early after addition of biotinylated pIgA, in agreement with reduced pIgA transcytosis reported in Yes knockout mice[15]. Thus, activation of EGFR is necessary and sufficient for enhancing transcytosis of pIgR.

Next, we tested the effect of expressing constitutively active EGFR on pIgA–pIgR transcytosis. Cells overexpressing wild-type EGFR formed polarized monolayers with basolateral EGFR (Supplementary Information, Fig. S3b, c), increased TER (Supplementary Information, Fig. S3d) and, as demonstrated above, hyperstimulated apical pIgA transcytosis (Fig. 4b). Conversely, cells expressing two different constitutively active EGFR mutants formed irregular monolayers and, despite maintaining apical–basal polarization, had pools of intracellular EGFR, either normal or slightly lowered TER and failed to increase pIgA transcytosis (Supplementary Information, Fig. S3b–d, f). Instead, cells expressing either of the constitutively active EGFR mutants (cell lines Δ3/A750P and L858R) had significantly increased basolateral secretory component in the absence of pIgA treatment (pIgR-expressing MDCK cells versus Δ3/A750P cells; 7.5 ± 0.6% versus 25.7 ± 1.9%, $n = 3$, $P < 0.001$; pIgR-expressing MDCK cells versus L858R cells; 7.5 ± 0.6% versus 19.5 ± 1.5%, $n = 3$, $P = 0.002$; all values represent the basolateral secretory component as a percentage of total labelled pIgR; Supplementary Information, Fig. S3e), suggesting that regulated, rather than constitutive EGFR activation is required to control pIgR transcytosis. EGFR knockdown significantly increased both apical and basal secretory component release in the absence of pIgA (apical secretory component release in cells expressing control shRNA versus cells expressing *EGFR* shRNA; 23.0 ± 1.3% versus 34.4 ± 1.3%, $n = 3$, $P = 0.003$; basolateral secretory component release in cells expressing control shRNA versus cells expressing *EGFR* shRNA; 9.7 ± 0.6% versus 16.9 ± 1.6%, $n = 3$, $P = 0.014$; all values represent the secretory component as a percentage of total labelled pIgR; Supplementary Information, Fig. S3e). These data reveal that EGFR, and its dynamic activation to an appropriate level by Yes, is required for the correct coupling of pIgR to transcytosis.

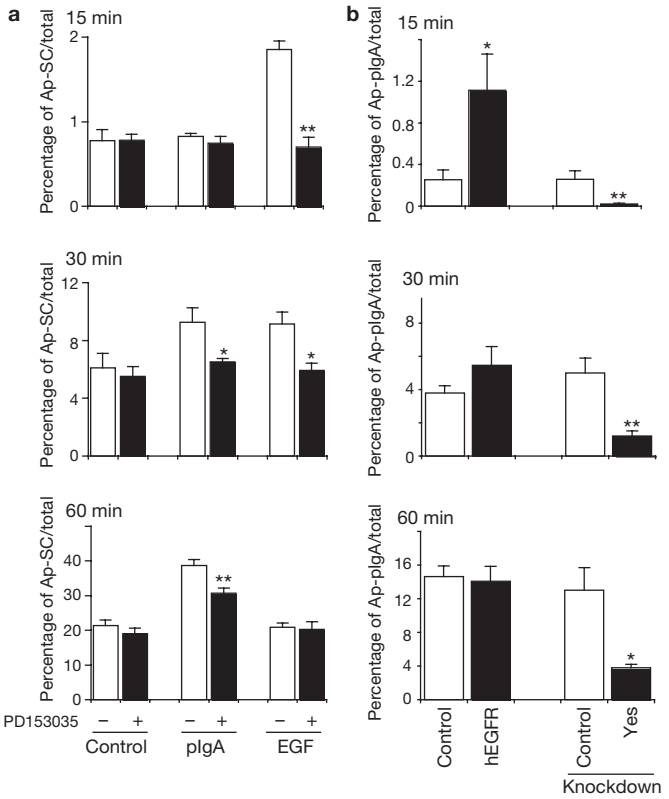

Figure 4 pIgA-stimulated pIgR transcytosis requires EGFR activity. (**a**) MDCK cells expressing pIgR were labelled with ^{35}S-cysteine and basolaterally treated with pIgA or EGF, with or without EGFR kinase inhibitor (PD153035) for the indicated times. Apically released secretory component (Ap-SC) is represented as a percentage of total labelled pIgR. Data are means ± s.e.m. Asterisk indicates $P < 0.05$ and double asterisks indicate $P < 0.001$, compared with cells not treated with PD153035 for the indicated treatment. Control cells with PD153035 treatment, $n = 8$, all others, $n = 6$. (**b**) MDCK cells expressing hEGFR and pIgR, MDCK cells expressing pIgR with Yes knockdown, and their respective controls, were basolaterally treated with biotinylated pIgA for indicated times, and the apically transcytosed pIgA (Ap-pIgA) was measured by ELISA. Data are represented as a percentage of the total pIgA and are means ± s.e.m. Asterisk indicates $P < 0.05$, double asterisks indicate $P < 0.001$, compared with respective control cells. Control and hEGFR-expressing cells, $n = 8$; control and Yes knockdown cells, $n = 12$.

Involvement of MAPKs in pIgR transcytosis

pIgA stimulated phosphorylation of EGFR predominantly on Tyr 992 and Tyr 1173 (Fig. 2d), coupling EGFR to the PLCγ1 and MAPK

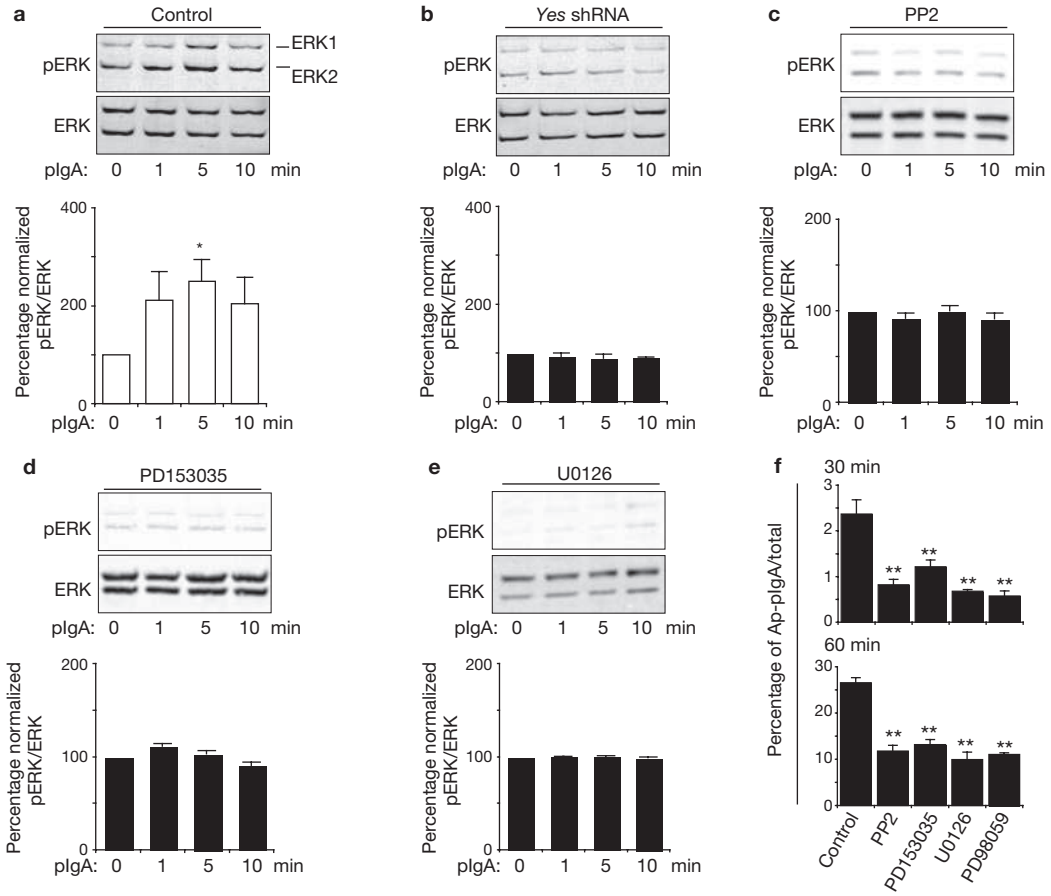

Figure 5 ERK phosphorylation induced by pIgA treatment is required for pIgA–pIgR transcytosis in MDCK cells expressing pIgR. (**a**–**f**) MDCK cells expressing pIgR were treated basolaterally with pIgA for the indicated times. Cells were left untreated (**a**, control), Yes was knocked down (**b**), or cells were treated with SFK inhibitor (PP2; **c**), EGFR inhibitor (PD153035; **d**) or MEK inhibitor (U0126; **e**). Top: cell lysates were analysed by immunoblotting with specific phosphorylated ERK (pERK) and ERK antibodies. Bottom: quantification of the phosphorylated ERK band intensities (normalized to the ERK bands). Asterisk (**a**) indicates $P < 0.03$, compared with control cells at 0 min, $n = 4$). (**f**) Cells were pre-treated for 2 h, and throughout the experiment, with the indicated inhibitors. Control cells were treated with DMSO. Apical pIgA transcytosis of basolaterally applied pIgA was analysed at the indicated times after addition of inhibitor. Data are represented as a percentage of the total pIgA and are means ± s.e.m. Double asterisks indicate $P < 0.001$, compared with control cells, $n = 4$).

(mitogen-activated protein kinase) pathways, respectively[22,23]. We previously reported a role for PLCγ1 in pIgR transcytosis[24] and therefore focused on MAPK. Immunoblotting of rat liver endosomes demonstrated that ERK1 and ERK2 were present (Supplementary Information, Fig. S5a). When pIgR-expressing MDCK cells were treated with pIgA, ERK phosphorylation was modestly, but significantly, induced on p44 and p42 ERK (increase in the ratio of phosphorylated ERK:ERK at 5 min of 149 ± 46%, compared with cells at 0 min of treatment; $n = 4$, $P < 0.03$; Fig. 5a). No increase in ERK phosphorylation occurred on pIgA stimulation in cells with Yes knockdown (Fig. 5b), or cells treated with SFK inhibitor (PP2; Fig. 5c), EGFR inhibitor (PD153035; Fig. 5d) or MEK (mitogen-activated protein kinase kinase) inhibitor (U0126; Fig. 5e). Levels of phophorylated ERK were further increased by pIgA stimulation in cells overexpressing hEGFR, compared with parental cells (compare Fig. 5a and Supplementary Information, Fig. S5b), corresponding to the enhanced transcytosis under this condition (Fig. 4b). Thus, pIgA induces ERK phosphorylation and this requires Yes, EGFR and MEK/ERK.

Inhibition of ERK activation by treatment with MEK inhibitors (U0126 or PD98059) significantly reduced pIgA transcytosis (2–4-fold at 30 min; 2–2.7-fold at 60 min; Fig. 5f) to levels observed with inhibition of SFK (PP2) or EGFR (PD153035; Fig. 5f). Notably, U0126, and to a lesser extent PD98059, partially inhibited transcytosis of pIgR even in the absence of pIgA (Supplementary Information, Fig. S5c, d), possibly owing to the involvement of MEK/ERK in constitutive pIgR transcytosis. These data suggest that the MEK/ERK pathway is involved in transcytosis of pIgA–pIgR.

Phosphorylation of FIP5 by ERK regulates pIgR transcytosis

Activation of EGFR and downstream ERK1 or ERK2 induced rapid pIgR transcytosis. We examined phosphoproteomic databases (www.phosida.com) for membrane trafficking proteins that are phosphorylated in response to EGF, and possess potential ERK phosphorylation sequences. We focused on FIP5, a Rab11-interacting protein[14], which possesses a conserved, canonical ERK phosphorylation site sequence (P-X-S/T-P, where X is any residue), at Ser 188 (Fig. 6a).

In MDCK cells, FIP5 is enriched in the ARE, where in conjunction with Rab11a, it regulates transcytosis of pIgA–pIgR to the apical plasma membrane[14]. Rab11a and FIP5 are on rat liver endosomes (Fig. 6b). We

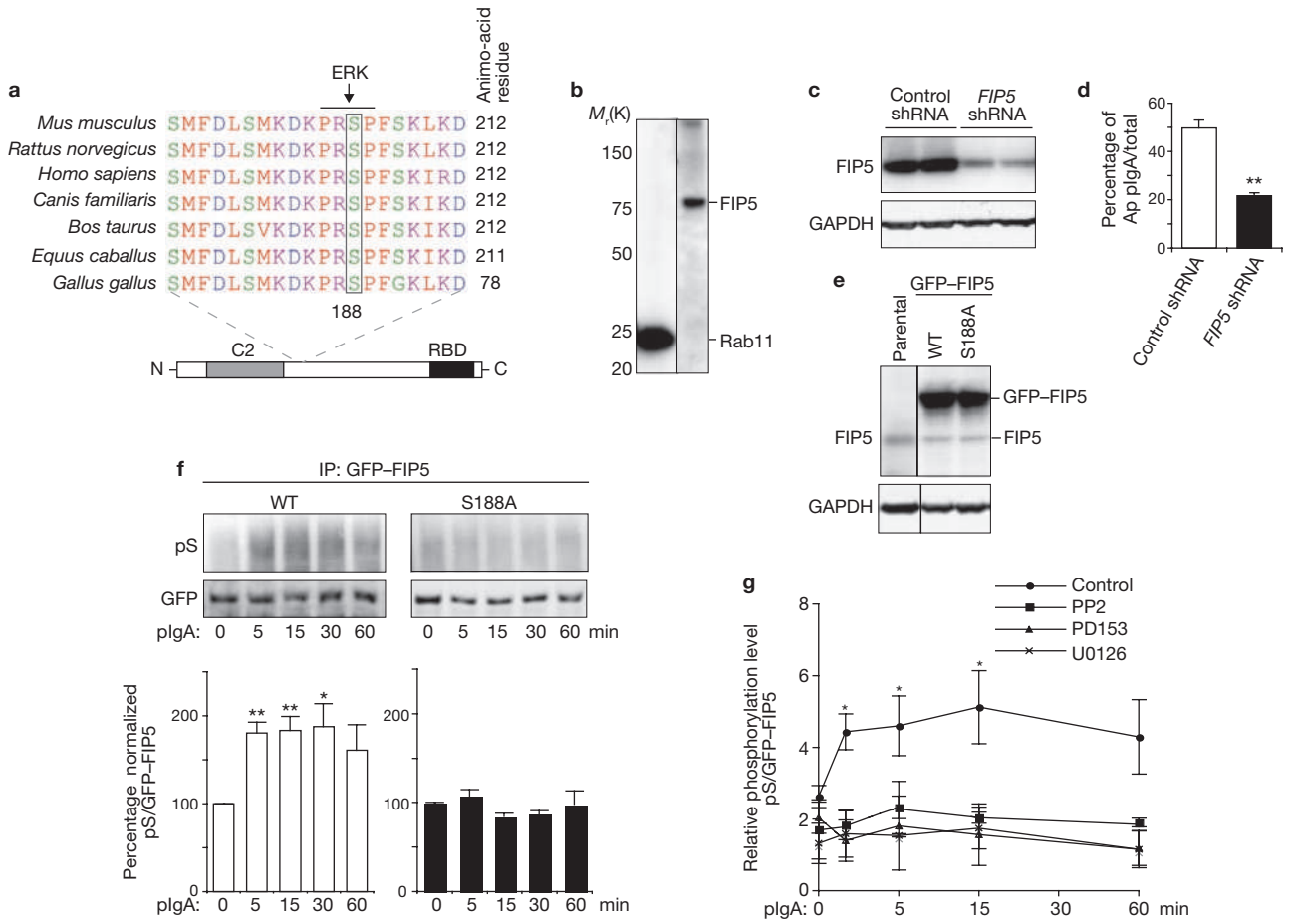

Figure 6 FIP5 phosphorylation is downstream of Yes–EGFR–ERK. (**a**) Comparison of the amino-acid sequences of FIP5 from the indicated species. A conserved ERK phosphorylation sequence at Ser 188 is indicated. Bottom: schematic representation of the FIP5 protein, indicating region compared at the top. N, amino-terminus; C, carboxyl terminus; RBD, Rab11-binding domain. (**b**) Immunoblotting of RRC fractions with antibodies against the indicated proteins. Box indicates splicing of bands from same gel. (**c**) Immunoblotting of the lysates from pIgR-expressing MDCK cells stably expressing *FIP5* shRNA and control cells expressing scrambled-sequence shRNA. Duplicate samples are presented. GAPDH; loading control. (**d**) pIgA transcytosis in pIgR-expressing MDCK cells stably expressing scrambled-sequence shRNA, or *FIP5* shRNA. Data are represented as a percentage of the total pIgA and are means ± s.e.m. Asterisks indicate $P < 0.001$, compared with control cells, $n = 4$. (**e**) Expression of FIP5 in MDCK cells. Levels of FIP5 were assessed in parental MDCK cells (left) and in cells overexpressing wild-type human FIP5 or an S188A mutant, both tagged with GFP. GAPDH, loading control. Box indicates splicing of bands from same gel. (**f**) MDCK cells stably expressing pIgR and GFP–FIP5 (wild type or S188A) were treated with pIgA for the indicated times. Top: cell lysates were immunoprecipitated with antibodies against GFP–FIP5 and then immunoblotted with antibodies specific to GFP–FIP5 and phosphorylated serine (pS). Bottom: intensity of the phosphorylated serine bands (normalized to the intensity of the GFP–FIP5 bands). Data are means ± s.e.m. Single asterisks indicate $P < 0.05$, double asterisks indicate $P < 0.001$, $n = 4$. (**g**) MDCK cells expressing pIgR and GFP–FIP5 were treated with pIgA for indicated times and with the indicated inhibitors (untreated cells, control). Cell lysates were immunoprecipitated for GFP–FIP5, resolved by SDS–PAGE, and immunoblotted for GFP–FIP5 or phosphorylated serine. Intensity of bands for phosphorylated serine were normalized to the intensity of GFP–FIP5 bands. Data are means ± s.e.m. Asterisks indicate $P < 0.05$, $n = 3$. Uncropped images of blots are shown in Supplementary Information, Fig. S7.

tested if FIP5 was required for pIgA–pIgR transcytosis, by knockdown of FIP5 (Fig. 6c, d). Indeed, pIgA transcytosis was significantly reduced by 56 ± 0.05% (30 min) on FIP5 knockdown, compared with control cells ($n = 4$, $P < 0.001$; Fig. 6d).

To examine whether FIP5 Ser 188 is a target for ERK, we stably expressed wild-type FIP5 or an S188A mutant, both tagged with GFP, in MDCK cells expressing pIgR (Fig. 6e). Densitometric analysis of the immunoblots revealed that GFP–FIP5 expression (wild type or the S188A mutant) was approximately 3.8-fold higher than endogenous FIP5. Stimulation of these cells with pIgA resulted in rapid phosphorylation of GFP–FIP5, as assessed by immunoprecipitation of GFP–FIP5 followed by immunoblotting with antibodies against phosphorylated serine (phosphorylated serine/GFP–FIP5 ratio, 87 ± 26% increase when compared with controls at 5 min; $n = 4$, $P < 0.001$, Fig. 6f). This phosphorylation peaked at 5–30 min and declined by 60 min (Fig. 6f). The phosphorylated serine-FIP5 band runs as a smear on an immunoblot, suggesting phosphorylation at multiple sites. In contrast, the phosphorylated serine signal was abolished in cells expressing GFP–FIP5^{S188A} (Fig. 6f), suggesting that Ser 188 is a key FIP5 phosphorylation residue. To confirm that FIP5 phosphorylation lay downstream of the Yes–EGFR–MAPK module, we treated wild-type cells with Yes (PP2), EGFR (PD153035) or MEK (U0126) inhibitors, before and during pIgA treatment. pIgA-induced GFP–FIP5 phosphorylation was abolished by these inhibitors (Fig. 6g).

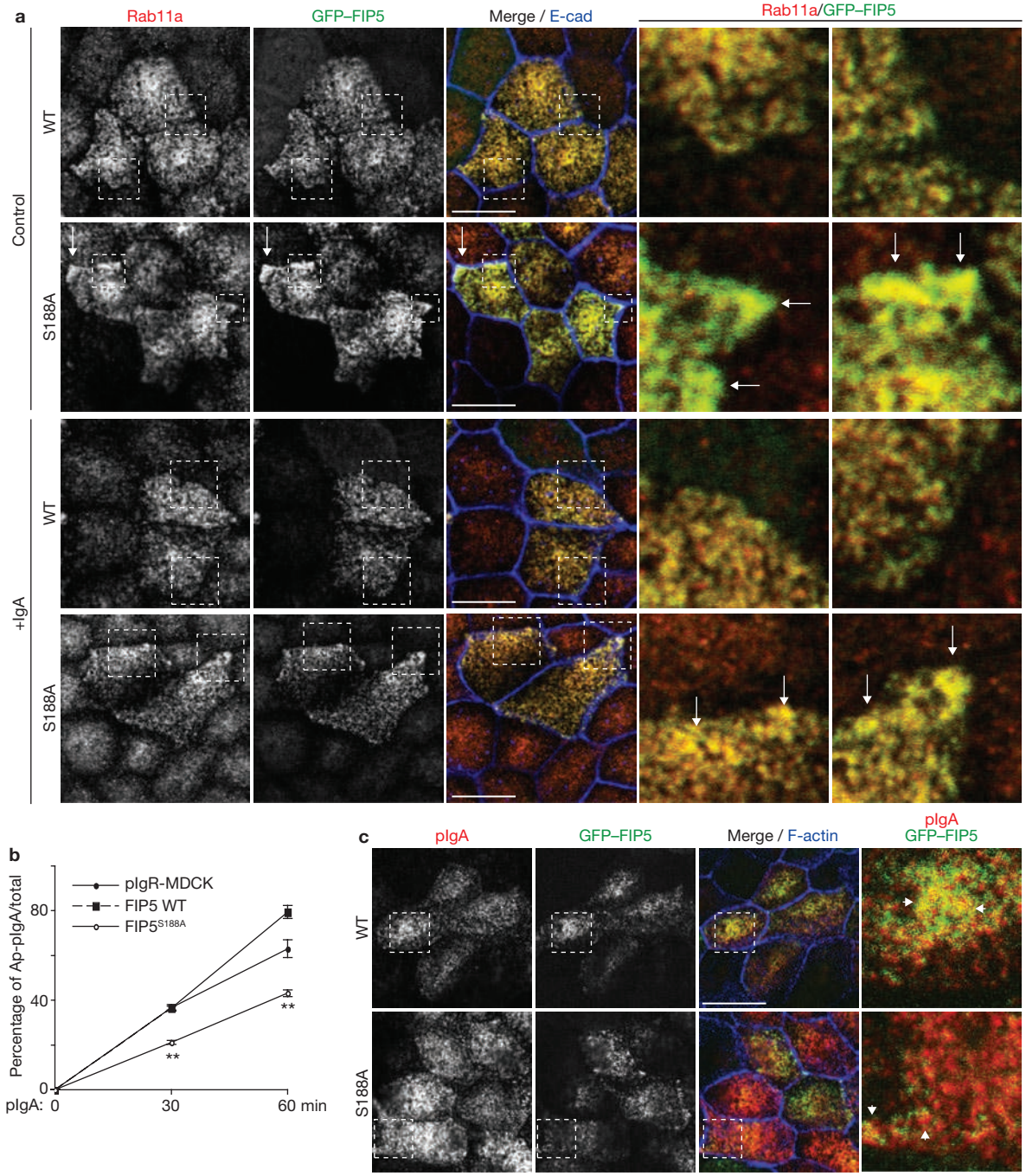

Figure 7 FIP5 Ser 188 phosphorylation regulates Rab11a localization and pIgA–pIgR transcytosis. (**a**) Filter-grown monolayers of MDCK cells expressing pIgR and stably expressing GFP–FIP5 (wild type or the S188A mutant, green) were immunostained for Rab11a (red) and E-cadherin (E-cad, blue) without (control) or with pIgA stimulation (15 min). Pairs of images on the right are higher-magnification images of boxed areas indicated in images on the left and demonstrate accumulation of Rab11a/FIP5-positive vesicles in the periphery of the sub-apical region of cells expressing GFP–FIP5^{S188A}, as indicated by arrows. (**b**) pIgA transcytosis assays were performed on parental MDCK cells expressing pIgR or MDCK cells expressing pIgR and GFP–FIP5 (wild type or the S188A mutant). Cells were treated with biotinylated pIgA, which was allowed to accumulate intracellularly, followed by incubation. Transcytosed pIgA was measured at the indicated times. Data are means ± s.e.m. Asterisks indicate $P < 0.001$, $n = 4$. (**c**) MDCK cells expressing pIgR and GFP–FIP5 (green; wild type; top, or the S188A mutant; bottom) were treated basolaterally with biotinylated pIgA, and immunostained for pIgA (red) and F-actin (blue) after 60 min of transcytosis. Yellow, arrowheads indicate overlap of pIgA and wild-type GFP–FIP5 in the centre of the sub-apical region of cells. Images on the right are higher-magnification images of boxed areas indicated in images on the left. Scale bars, 20 μm.

Rab11-FIP mutants in *Drosophila melanogaster* delocalize Rab11a and myosin Vb, both of which regulate pIgA–pIgR transcytosis[13,25,26]. We examined whether expression of GFP–FIP5^{S188A} affected Rab11a localization in polarized monolayers. Similarly to previous reports[13,14], Rab11a localized to vesicles clustered in the middle of the sub-apical region of cells, largely overlapping with GFP–FIP5 (Fig. 7a). pIgA stimulation dispersed FIP5-Rab11a vesicles through the sub-apical region. In cells expressing GFP–FIP5^{S188A}, both Rab11a and the FIP5 mutant co-labelled vesicles in

the periphery of cells, with or without pIgA stimulation (Fig. 7a, arrows). This suggests that ERK-regulated phosphorylation of FIP5 regulates the polarized distribution of Rab11a-FIP5-labelled vesicles.

To determine whether FIP5 Ser 188 phosphorylation is required for transcytosis, cells expressing GFP– FIP5 (wild type versus the S188A mutant) were treated with biotinylated pIgA at the basolateral surface, before incubation to allow pIgA to accumulate intracellularly[21]. pIgA transcytosis was increased in cells overexpressing wild-type GFP–FIP5 at 60 min. In contrast, pIgA transcytosis was strikingly reduced in cells expressing GFP–FIP5^{S188A}, compared with wild-type GFP–FIP5 or parental pIgR-expressing MDCK cells (Fig. 7b, wild-type FIP5- versus FIP5^{S188A}-expressing cells at 30–60 min, $n = 4$, $P < 0.001$; wild-type FIP5-expressing cells versus control at 30–60 min, $n = 4$, 30 min, $P > 0.5$ and 60 min, $P < 0.016$). Accordingly, analysis of pIgA localization in cells expressing GFP–FIP5^{S188A}, through immunofluorescence microscopy or immunoblotting of cell lysates, indicated intracellular accumulation of pIgA, compared with cells expressing wild-type GFP–FIP5 at 60 min (Fig. 7c and Supplementary Information, Fig. S6a, b), at which time the majority of pIgA has normally transcytosed (Fig. 7b). In contrast to cells expressing wild-type GFP–FIP5, which displayed strong overlap with pIgA in vesicles, GFP–FIP5^{S188A}-expressing cells possess pIgA in vesicles distributed throughout the sub-apical cytoplasm, much of which did not overlap with the FIP5 mutant. These data reveal that ERK-regulated phosphorylation of FIP5 is critical for pIgA transcytosis.

DISCUSSION

Our data suggest a pathway where pIgA binding to pIgR activates Yes, followed by activation of EGFR and then the MEK–ERK module (presumably through Ras and Raf), which culminates in phosphorylation of FIP5, control of Rab11a localization and stimulation of transcytosis (Fig. 8a). Earlier work indicated that regulation of pIgA transcytosis also involves calcium, kinases (protein kinase C; PKC and phosphatidylinositol 3-kinase; PI3Kinase), numerous Rabs (Rab3b, Rab5, Rab11a, Rab17 and Rab25), retromer and signals in the pIgR cytoplasmic domain[4,5,27–30]. Thus, this cascade is part of a complex network governing transcytosis.

pIgR, EGFR and Yes formed a complex in sub-apical endosomes, which were devoid of the ARE marker Rab11a, suggesting that the complex may occur in apically located common recycling endosomes (CREs), before ARE entry (Fig. 8b). pIgA stimulated dispersal of the complex, concomitant with apical transcytosis of pIgA–pIgR, which occurs through the ARE under control of Rab11a[21,31]. EGFR knockdown not only attenuated pIgA-induced pIgR transcytosis, but also increased transport of non-receptor-bound pIgR to both the apical and basolateral surfaces, suggesting a fundamental requirement for EGFR in regulating pIgR transport to the apical surface.

Rab11a and FIP5 regulate pIgA transcytosis[14,31]. Here, we demonstrate that ERK phosphorylation on FIP5 Ser 188 is crucial for efficient pIgA–pIgR transcytosis. pIgA-induced FIP5 phosphorylation is blocked by inhibitors of SFK, EGFR or MEK. Expression of a FIP5^{S188A} mutant disrupted polarized distribution of pIgA and Rab11a and led to co-accumulation of Rab11a/FIP5-labelled vesicles in the periphery of the sub-apical region, suggesting that Ser 188 phosphorylation controls localization of FIP5 and Rab11a. FIP5^{S188A} also functioned as a dominant-negative inhibitor of pIgA-induced transcytosis, suggesting that this EGFR/MEK/ERK target is a critical residue in the regulation of transcytosis.

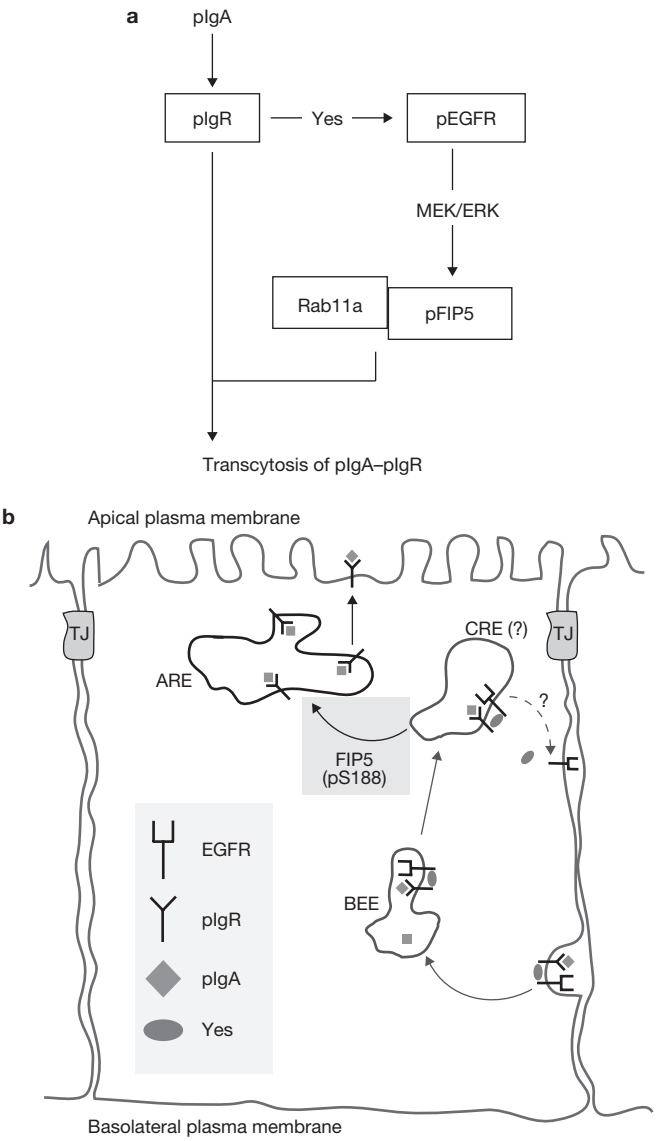

Figure 8 A kinase cascade regulating pIgR transcytosis. (**a**) A Yes–EGFR–ERK–FIP5 signalling cascade controls pIgA–pIgR transcytosis in epithelial cells. pIgA stimulates pIgR activation, which associates with Yes, and directs phosphorylation of EGFR. Active phosphorylated EGFR, presumably through Ras/Raf, activates MEK/ERK, which in turn phosphorylates FIP5 on Ser 188 (pFIP5). FIP5, phosphorylated on Ser 188, functions with Rab11a to regulate transcytosis of pIgA–pIgR complexes. (**b**) FIP5 phosphorylation controls polarized distribution of Rab11a and pIgA transcytosis. A schematic representation of how pIgR–Yes–EGFR complexes are internalized and passaged through basolateral early endosomes (BEEs) to sub-apical endosomes, presumably the common recycling endosome (CREs). pIgA causes the disruption of the pIgR–Yes–EGFR complex in endosomes. The EGFR–MEK/ERK cassette phosphorylates FIP5 on Ser 188 (pS188), which controls re-distribution of Rab11a/FIP5 vesicles from the periphery to the centre of the apical region of cells. This may represent the transition from the CRE to the apical recycling endosome (ARE). From here EGFR may be recycled to the basolateral plasma membrane. pIgA–pIgR complexes are delivered to the ARE, from where they are delivered to the apical plasma membrane. Thus the EGFR–MEK/ERK cassette represents an unappreciated regulator of transport through the transcytotic pathway. TJ; tight junctions.

EGFR activation by tyrosine phosphorylation may regulate this network by coupling EGFR to numerous effectors with SH2 domains[32–34]. For example, EGFR phosphorylated at Tyr 992 phosphorylates and

activates PLCγ[35,36]. Phosphorylation of PLCγ1 increases in MDCK cells on pIgA binding[24]. The resultant phospholipid hydrolysis leads to activation of PKC and elevation of intracellular free calcium; both promote pIgR transcytosis[37,38]. We now show that pIgA binding leads to phosphorylation of EGFR mainly at Tyr 992, Tyr 1173 and Tyr 845. The role of ERKs in pIgA transcytosis was focused on because ERK can be activated by phosphorylation of EGFR Tyr 1173/Tyr 992 through the Ras–Raf–MEK pathway[39–41]. ERK is abundant in rat liver endosomes and we show that EGFR functions, at least partly, by coupling pIgR to ERK, which is activated rapidly after pIgA stimulation. pIgA-induced phosphorylation of ERK was blocked by depleting or inhibiting either Yes or EGFR, suggesting that EGFR activates the MEK/ERK pathway in pIgR-containing endosomes.

This pathway links kinases that are traditionally viewed as regulating development (EGFR–MAPK–ERK)[42] with regulators of membrane traffic (Rab11a and FIP5). An explanation for this unusual connection is that the levels of phosphorylation and activation of these signalling components by pIgA are lower than usually seen in regulation of development (though statistically significant and reproducible). Indeed, constitutive EGFR activation perturbed, rather than promoted, transcytosis. Notably, ERK has also been found to directly phosphorylate and control the function of protrudin, another Rab11-interacting protein that regulates polarized endocytic sorting[43]. Furthermore, inhibition of the MEK–ERK pathway perturbs endosome morphology and recycling of molecules in ARF6-positive recycling vesicles[40]. Thus, in addition to the bistable regulation of developmental processes often associated with EGFR and kinase cascades, our data support an emerging model that endocytic machinery may be a common, but unappreciated, target of ERKs regulating membrane traffic in diverse contexts. Regulation of pIgA transcytosis involves transmission of information across the cell; ERK signalling is suited for such long distance signal transmission[44].

Regulation of membrane traffic is a central issue in cell biology. Indeed, many types of physiological adaptation as well as most developmental events involve regulation of membrane traffic[45]. One general type of traffic regulation is that the level of cargo can regulate its own transport. For example, an increase in the amount of newly synthesized secretory protein in the endoplasmic reticulum can lead to an increase in the amount of chaperones needed to properly fold the cargo, as well as in the amount of vesicular traffic leaving the endoplasmic reticulum[46]. The ability of the pIgR to increase its transcytosis in response to an increase in the amount of pIgA is a good model of this type of autoregulation.

Autoregulation of pIgA transcytosis is probably medically important. In response to mucosal infection, pIgA production can rapidly increase and autoregulation provides for its efficient transport into secretions. pIgA often forms a complex with antigen[47] and failure to adequately transport such antigen–antibody complexes may lead to their pathological deposition, such as in IgA nephropathy, a major cause of kidney failure worldwide[48]. Moreover, in IgA nephropathy, IgA complexes are abnormally deposited in renal glomeruli. This might cause abnormal activation of signalling by EGFR (or members of the EGFR family) leading to pathological proliferation, a hallmark of IgA nephropathy. The regulation of transcytosis by EGFR provides a rapid, post-transcriptional mechanism for coordinating response to infection or injury with mucosal immunity. pIgR is also transcriptionally upregulated by several cytokines, providing a complementary mechanism to coordinate pIgA transcytosis with mucosal immunity[49]. □

METHODS

Methods and any associated references are available in the online version of the paper at http://www.nature.com/naturecellbiology/

Note: Supplementary Information is available on the Nature Cell Biology website

ACKNOWLEDGEMENTS

We thank Mostov lab members and M. von Zastrow for valuable input and critical reading of the manuscript. We thank K. Young and T. Evans for technical assistance. We acknowledge J. Brugge, J. Goldenring, J. Gordon, M. McCaffrey, J. Peppard, M. Sudol, D. C. James, Q. Fan and J. -P. Vaerman for reagents. This work was supported by NIDDK UCSF Liver Center Pilot Project to the Molecular Structure Core of the Liver Center at UCSF (NIH P30 DK026743; awarded to T.S.), a Susan G Komen Foundation Fellowship (to D.M.B.), a DOD Lung Cancer Concept Award (to A.D.), NIH NCRR 01614 (to A.L.B.), NIH R01EB001987 (to K.M.S.), and R01AI25144, R01DK083330 and R01DK074398 (to K.E.M.).

AUTHOR CONTRIBUTIONS

T.S., D.M.B., F.L. and K.E.M. designed and analysed the experiments. T.S., D.M.B., M.V. and K.C.H. performed the experiments. A.D., D.J.E, S.M.U., K.M.S. and A.L.B. provided reagents. T.S., D.M.B. and K.E.M. wrote the manuscript. D.M.B. and K.E.M. supervised the project.

COMPETING FINANCIAL INTERESTS

The authors declare no competing financial interests.

Published online at http://www.nature.com/naturecellbiology
Reprints and permissions information is available online at http://npg.nature.com/reprintsandpermissions/

1. Mellman, I. & Nelson, W. J. Coordinated protein sorting, targeting and distribution in polarized cells. *Nat. Rev. Mol. Cell Biol.* **9,** 833–845 (2008).
2. Weisz, O. A. & Rodriguez-Boulan, E. Apical trafficking in epithelial cells: signals, clusters and motors. *J. Cell Sci.* **122,** 4253–4566 (2009).
3. Sorkin, A. & von Zastrow, M. Endocytosis and signalling: intertwining molecular networks. *Nat. Rev. Mol. Cell Biol.* **10,** 609–622 (2009).
4. Mostov, K. E., Su, T. & ter Beest, M. Polarized epithelial membrane traffic: conservation and plasticity. *Nat. Cell Biol.* **5,** 287–293 (2003).
5. Rojas, R. & Apodaca, G. Immunoglobulin transport across polarized epithelial cells. *Nat. Rev. Mol. Cell Biol.* **3,** 944–956 (2002).
6. Song, W., Bomsel, M., Casanova, J., Vaerman, J.-P. & Mostov, K. E. Stimulation of transcytosis of the polymeric immunoglobulin receptor by dimeric IgA. *Proc. Natl Acad. Sci. USA* **91,** 163–166 (1994).
7. Giffroy, D. *et al. In vivo* stimulation of polymeric Ig receptor-transcytosis by circulating polymeric IgA in rat liver. *Int. Immunol.* **10,** 347–354 (1998).
8. Bomsel, M. & Mostov, K. Role of heterotrimeric G proteins in membrane traffic. *Mol. Biol. Cell* **3,** 1317–1328 (1992).
9. Kaetzel, C. S. The polymeric immunoglobulin receptor: bridging innate and adaptive immune responses at mucosal surfaces. *Immunol. Rev.* **206,** 83–99 (2005).
10. Tuma, P. L. & Hubbard, A. L. Transcytosis: crossing cellular barriers. *Physiol. Rev.* **83,** 871–932 (2003).
11. Song, W., Apodaca, G. & Mostov, K. Transcytosis of the polymeric immunoglobulin receptor is regulated in multiple intracellular compartments. *J. Biol. Chem.* **269,** 29474–29480 (1994).
12. van IJzendoorn, S. C. D., Tuvim, M. J., Weimbs, T., Dickey, B. F. & Mostov, K. E. Direct interaction between Rab3b and the polymeric immunoglobulin receptor controls ligand-stimulated transcytosis in epithelial cells. *Dev. Cell* **2,** 219–228 (2002).
13. Casanova, J. E. *et al.* Association of Rab25 and Rab11a with the apical recycling system of polarized Madin-Darby canine kidney cells. *Mol. Biol. Cell* **10,** 47–61 (1999).
14. Prekeris, R., Klumperman, J. & Scheller, R. H. A Rab11/Rip11 protein complex regulates apical membrane trafficking via recycling endosomes. *Mol. Cell* **6,** 1437–1448 (2000).
15. Luton, F., Vergés, M., Vaerman, J.-P., Sudol, M. & Mostov, K. E. The src family protein tyrosine kinase p62*yes* controls polymeric IgA transcytosis *in vivo*. *Mol. Cell* **4,** 627–632 (1999).
16. Shah, K., Liu, Y., Deirmengian, C. & Shokat, K. M. Engineering unnatural nucleotide specificity for Rous sarcoma virus tyrosine kinase to uniquely label its direct substrates. *Proc. Natl Acad. Sci. USA* **94,** 3565–3570 (1997).
17. Liu, Y., Shah, K., Yang, F., Witucki, L. & Shokat, K. M. Engineering Src family protein kinases with unnatural nucleotide specificity. *Chem. Biol.* **5,** 91–101 (1998).
18. Vergés, M., Havel, R. J. & Mostov, K. E. A tubular endosomal fraction from rat liver: biochemical evidence of receptor sorting by default. *Proc. Natl Acad. Sci. USA* **18,** 10146–10151 (1999).
19. Bishop, A. C. *et al.* A chemical switch for inhibitor-sensitive alleles of any protein kinase. *Nature* **407,** 395–401 (2000).
20. Mullock, B. M., Jones, R. S. & Hinton, R. H. Movement of endocytic shuttle vesicles from the sinusoidal to the bile canalicular face of hepatocytes does not depend on occupation of receptor sites. *FEBS Lett.* **113,** 201–205 (1980).
21. Apodaca, G., Katz, L. A. & Mostov, K. E. Receptor-mediated transcytosis of IgA in MDCK cells via apical recycling endosomes. *J. Cell Biol.* **125,** 67–86 (1994).

22. Jorissen, R. N. *et al.* Epidermal growth factor receptor: mechanisms of activation and signalling. *Exp. Cell Res.* **284,** 31–53 (2003).
23. Haugh, J. M. Localization of receptor-mediated signal transduction pathways: the inside story. *Mol. Interv.* **2,** 292–307 (2002).
24. Luton, F., Cardone, M. H., Zhang, M. & Mostov, K. E. Role of tyrosine phosphorylation in ligand-induced regulation of transcytosis of the polymeric Ig receptor. *Mol. Biol. Cell* **9,** 1787–1802 (1998).
25. Li, B. X., Satoh, A. K. & Ready, D. F. Myosin V, Rab11 and dRip11 direct apical secretion and cellular morphogenesis in developing *Drosophila* photoreceptors. *J. Cell Biol.* **177,** 659–669 (2007).
26. Lapierre, L. A. *et al.* Myosin Vb is associated with plasma membrane recycling systems. *Mol. Biol. Cell* **12,** 1843–1857 (2001).
27. Hansen, S. H., Olsson, A. & Casanova, J. E. Wortmannin, an inhibitor of phosphoinositide 3-kinase, inhibits transcytosis in polarized epithelial cells. *J. Biol. Chem.* **270,** 28425–28432 (1995).
28. Vergés, M. *et al.* The mammalian retromer regulates transcytosis of the polymeric immunoglobulin receptor. *Nat. Cell Biol.* **6,** 763–769 (2004).
29. Verges, M., Sebastian, I. & Mostov, K. E. Phosphoinositide 3-kinase regulates the role of retromer in transcytosis of the polymeric immunoglobulin receptor. *Exp. Cell Res.* **313,** 707–718 (2007).
30. Luton, F., Hexham, M. J., Zhang, M. & Mostov, K. E. Identification of a cytoplasmic signal for apical transcytosis. *Traffic* **10,** 1128–1142 (2009).
31. Wang, X., Kumar, R., Navarre, J., Casanova, J. E. & Goldenring, J. R. Regulation of vesicle trafficking in Madin-Darby canine kidney cells by Rab11a and Rab25. *J. Biol. Chem.* **275,** 29138–29146 (2000).
32. Pawson, T. Specificity in signal transduction: from phosphotyrosine-SH2 domain interactions to complex cellular systems. *Cell* **116,** 191–203 (2004).
33. Thelemann, A. *et al.* Phosphotyrosine signaling networks in epidermal growth factor receptor overexpressing squamous carcinoma cells. *Mol. Cell Proteomics* **4,** 356–376 (2005).
34. Wu, S. L. *et al.* Dynamic profiling of the post-translational modifications and interaction partners of epidermal growth factor receptor signaling after stimulation by epidermal growth factor using extended range proteomic analysis (ERPA). *Mol. Cell Proteomics* **5,** 1610–1627 (2006).
35. Rotin, D. *et al.* SH2 domains prevent tyrosine dephosphorylation of the EGF receptor: identification of Tyr992 as the high-affinity binding site for SH2 domains of phospholipase Cγ. *EMBO J.* **11,** 559–567 (1992).
36. Vega, Q. C. *et al.* A site of tyrosine phosphorylation in the C terminus of the epidermal growth factor receptor is required to activate phospholipase C. *Mol. Cell Biol.* **12,** 128–135 (1992).
37. Cardone, M. H., Smith, B. L., Song, W., Mochley-Rosen, D. & Mostov, K. E. Phorbol myristate acetate-mediated stimulation of transcytosis and apical recycling in MDCK cells. *J. Cell Biol.* **124,** 717–727 (1994).
38. Cardone, M. H. *et al.* Signal transduction by the polymeric immunoglobulin receptor suggests a role in regulation of receptor transcytosis. *J. Cell Biol.* **133,** 997–1005 (1996).
39. McKay, M. M. & Morrison, D. K. Integrating signals from RTKs to ERK/MAPK. *Oncogene* **26,** 3113–3121 (2007).
40. Robertson, S. E. *et al.* Extracellular signal-regulated kinase regulates clathrin-independent endosomal trafficking. *Mol. Biol. Cell* **17,** 645–657 (2006).
41. Rubinfeld, H. & Seger, R. The ERK cascade: a prototype of MAPK signaling. *Mol. Biotechnol.* **31,** 151–174 (2005).
42. Pelkmans, L. *et al.* Genome-wide analysis of human kinases in clathrin- and caveolae/raft-mediated endocytosis. *Nature* **436,** 78–86 (2005).
43. Shirane, M. & Nakayama, K. I. Protrudin induces neurite formation by directional membrane trafficking. *Science* **314,** 818–821 (2006).
44. Kholodenko, B. N., Hancock, J. F. & Kolch, W. Signalling ballet in space and time. *Nat. Rev. Mol. Cell Biol.* **11,** 414–426 (2010).
45. Lecuit, T. & Pilot, F. Developmental control of cell morphogenesis: a focus on membrane growth. *Nat. Cell Biol.* **5,** 103–108 (2003).
46. Zhang, K. & Kaufman, R. J. Signaling the unfolded protein response from the endoplasmic reticulum. *J. Biol. Chem.* **279,** 25935–25938 (2004).
47. Lamm, M. E. Current concepts in mucosal immunity IV. How epithelial transport of IgA antibodies relates to host defense. *Am. J. Physiol. Gastrointest. Liver Physiol.* **274,** G614–G617 (1998).
48. Kaetzel, C. & Mostov, K. E. *Immunoglobulin transport and the polymeric immunoglobulin receptor* 211–250 (Academic, 2005).
49. Strugnell, R. A. & Wijburg, O. L. The role of secretory antibodies in infection immunity. *Nat. Rev. Microbiol.* **8,** 656–667 (2010).

DOI: 10.1038/ncb2118

METHODS

Reagents and antibodies. The ATP analogues, N^6-(benzyl) ATP and [γ-^{32}P] N^6-(benzyl) ATP, the tyrosine kinase substrate peptide IYGEFKKK, and the specific inhibitor of mutated Yes kinase, 1-NM-PP1, were synthesized as previously described[19,50–52]. L-[^{35}S]cysteine was purchased from PerkinElmer (Boston, MA). The inhibitor PP2 (used at 10 μM, or indicated concentrations), its inactive analogue PP3 (used at indicated concentrations), PD153035 (used at 2 μM) and PD98059 (used at 50 μM) were purchased from Calbiochem, U0126 (used at 10 μM) was from Promega. pIgA was provided by J. -P. Vaerman (Catholic University of Louvain, Belgium) and biotinylated using sulfo-NHS-LC-biotin (Pierce). EGF (used at 100 ng ml^{-1}) was from Invitrogen. Purified polymeric rat pIgA (91C) was provided by J. Peppard (Wayne State University, USA). Biotinylated HRP was from Zymed, and Streptavidin was purchased from Sigma.

Primary antibodies: mouse anti-Yes, clones 2.7 and 1373.7, a gift from J. Brugge (Harvard Medical School, USA; immunoblotting, 1:1,000; immunofluorescence microscopy, 1:100; immunoprecipitation, 1 μg per sample); anti-phosphorylated tyrosine (4G10), from Upstate (immunoblotting, 1:1,000); phosphorylated Tyr-100 antibody, from Cell Signalling (immunoblotting, 1:1,000); rabbit anti-Yes, from Upstate (immunoblotting, 1:1,000; immunoprecipitation, 1 μg); sheep anti-EGFR, from Abcam and Fitzgerald (both antibodies: immunoblotting, 1:1,000; immunofluorescence microscopy, 1:200; immunoprecipitation, 1μg); rabbit anti-EGFR, mouse anti-pERK, rabbit anti-ERK1/2 and rabbit anti-myosin light chain (MLC), from Santa Cruz (immunoblotting for all antibodies, 1:1,000); rabbit anti-phospho-EGFR kit, from Cell Signalling (immunoblotting, 1:1,000); mouse anti-biotin, from Jackson ImmunoResearch (immunoblotting, 1:1,000); rabbit anti-Rab11-FIP5 (pp75), provided by E. Chan (University of Florida, USA, through J. Goldenring, Vanderbilt University, USA; immunoblotting, 1:1,000); rabbit anti-GFP, from Molecular Probes (immunoprecipitation, 1 μg per sample); mouse anti-GFP from Roche Diagnostics (immunoblotting, 1:1,000); mouse anti-phosphorylated serine antibodies, from Calbiochem (immunoblotting, 1:500); rabbit anti-ERK conjugated to Alexa Fluor 680 (1:10,000); guinea pig anti-pIgR secretory component and sheep anti-secretory component, isolated in our lab (immunoblotting, 1:1,000; immunofluorescence microscopy, 1:300; immunoprecipitation, 1μg per sample); rabbit anti-pIgR (antibody 816), from J. -P. Vaerman (immunoblotting, 1:1,000; immunoprecipitation, 1μg per sample); rabbit anti-Rab11, from Zymed Laboratories (immunoblotting, 1:1,000; immunofluorescence microscopy, 1:100); mouse anti-GAPDH from Chemicon (immunoblotting, 1:10,000). Secondary antibodies for immunoblotting: Alexa 680 conjugated antibodies, from Molecular Probes (1:4,000); IRDye800 conjugated antibodies, from Rockland (1:3,000); HRP conjugated antibodies, from Jackson ImmunoResearch (1:10,000). Secondary antibodies for immunofluorescence microscopy staining: all Alexa dye-conjugated secondary antibodies were from Molecular Probes (1:200).

Plasmid construction, site-directed mutagenesis, protein expression and protein purification. The murine Yes cDNA was transferred from the vector pMIK-Neo (provided by M. Sudol, Mount Sinai School of Medicine, USA) to pGEX4T-2 (Amersham Pharmacia). For cloning of mutant Yes (T346G) GST fusion protein, the full-length Yes coding sequence was constructed using two-step PCR. The *Saccharomyces cerevisiae N*-myristoyltransferase expression vector (pBB131) was provided by J. I. Gordon (Washington University, USA)[53]. The myristoylated mutant Yes GST fusion protein (Yes-GTM) was made by co-transformation of pGEX-4T containing mutant Yes and pBB131 containing the yeast *N*-myristoyltransferase into BL21-CodonPlus-RIL strain (Stratagene) as previously described[54]. Yes-GTM was purified by glutathione–Sepharose beads, as described[55]. pEGFP–C1-Rab11-FIP5 plasmid[56] was provided by M.W. McCaffrey (University College Cork, Ireland) and mutagenesis was performed by standard methods.

Cell lines, transfection and RNA interference. MDCK cell lines expressing rabbit pIgR were developed in our laboratory[57]. pWZLhygro-hEGFR wild-type, (provided by D. James and Q. Fan, UCSF, USA) and pBabe-puro-EGFR (Δ3/750P and L858R variants[58]) viral vectors were used for EGFR variant expression. Amphotropic Phoenix cells (ATCC) were transfected with the viral vectors for virus production and viral supernatant was used to infect pIgR-expressing MDCK cells. Lentiviral shRNA constructs were used to target canine Yes (pPRIME vector[59]), FIP5 (pLKO.1-puro vector[60]), or EGFR (pLKO.1-blasticidin; developed in our laboratory). The RNAi sequences were as follows: *Yes* 1, forward, 5′-AGGGTGACAATGTGAAACACTA-3′, reverse 3′-TAGTGTTTCACATTGTCACCCC-5′; *Yes* 2, forward, 5′-AGGTGACAATGTGAAACACTAC-3′, reverse 3′-GTAGTGTTTCACATTGTCACCC-5′; *FIP5*, 5′-(AA)TGGGAGCCACATTTACAAT-3′; *EGFR*, 5′-(AA)TCCCGTCTATCACAATCAG- 3′. 293FT cells (Invitrogen) were co-transfected with the viral vector, and ViraPower Packaging mix (Invitrogen) for lentivirus production. The viral supernatant was used to infect pIgR-expressing MDCK cells, and stable knockdown cells were selected with appropriate antibiotic. Wild type and S188A mutant hEGFR-Rab11-FIP5 plasmids were transfected into pIgR-expressing MDCK cells, selected by G418, then sorted by fluorescence-activated cell sorting (FACS) to make stable lines. Protein knockdown level was assessed by immunoblotting followed by densitometric analysis of the bands, and calculating as follows: (control – knockdown)/control × 100%.

For all transcytosis assays, cell monolayers were grown on polycarbonate Transwell filters (plated 5 × 10^5 cells per 12 mm filter) for 4 days. pIgA binding assays using 0.3 mg ml^{-1} human pIgA were performed on monolayers pre-incubated in serum-free medium for 6–16 h.

pIgA injection and isolation of a rat liver endosome fraction. Male Sprague-Dawley rats (200–250 g) were from Charles River Laboratories, USA. Animals were treated according to the protocols approved by the UCSF Laboratory Animal Resource Center. Rat pIgA (10 mg per rat) was injected through a femoral vein 1 min before endosome isolation[15]. Rat liver endosome fractionation was performed as previously described, but here rats were not pre-treated with oestrogen and low-density lipoprotein (LDL)[61]. All steps were performed at 4 °C. The endosome fraction previously termed receptor-recycling compartment (RRC) was used for this study[18]. Protein concentration of endosome fractions was determined by the BCA (bicinchoninic acid) method (Pierce).

Protein kinase assays. For measuring Yes-GTM activity, phosphorylation of the peptide substrate IYGEFKKK was determined by *in vitro* kinase assay, as previously described[16,62].

To identify the tyrosine-phosphorylated Yes-GTM substrates, 25 μg RRC fraction was incubated with 0.5 μg Yes-GTM in the presence or absence of ATP analogues. The kinase reaction mixture had a final volume of 30 μl and contained 10 mM Hepes at pH 7.4, 50 mM NaCl, 10 mM $MnC1_2$, 10 mM $MgCl_2$, 0.2 mM sodium orthovanadate, 1 mM NaF, 0.5 μg Yes-GTM, and 2.5 μCi [γ-^{32}P] N^6-(benzyl) ATP or 0.1 mM N^6-(benzyl) ATP. After 4 min, or as indicated, the reaction was stopped by adding 15 μl of SDS (sodium dodecyl sulfate)-sample buffer containing DTT (dithiothreitol). The samples were then processed for SDS–PAGE . The gels were scanned in a phosphorimager for radioactively labelled ATP analogues. In experiments with unlabelled ATP analogues, the separated proteins were transferred onto PVDF (polyvinylidene fluoride) membranes for immunoblotting.

Affinity purification of phosphotyrosine proteins for mass spectrometry. The RRC endosome fraction (0.5–0.7 mg protein) was incubated with 5 μg Yes-GTM with or without 0.1 mM N^6-(benzyl) ATP. Then, endosomes were precipitated by centrifugation and solubilized in a solution containing 0.5% NP40, 20 mM Hepes at pH 7.4, 125 mM NaCl, 1 mM NaF, 1 mM sodium orthovanadate and protease inhibitors. Tyrosine phosphorylated proteins were immunoprecipitated by anti-phosphorylated tyrosine (4G10 antibody)-coupled protein A beads and separated in 7.5% (v/v) SDS–PAGE gels. Protein gels were silver stained and the bands of interest were sequenced by mass spectrometry as previously described[28].

Immunoblotting and co-immunoprecipitation. For immunoblotting, equal amounts of protein from endosomes, or cell lysates (10–20 μg protein per lane), were processed for SDS–PAGE. PVDF membranes were blocked using LI-COR blocker buffer (LI-COR Biosciences). Protein bands were visualized by Odyssey NIR Imager scanner (LI-COR Biosciences) or enhanced chemiluminescence (ECL; Thermo Scientific). Co-immunoprecipitation was performed as described[28]. For immunoprecipitation, 30–50 μg of protein from endosomes, or 1–1.5 mg of protein from cell lysate, per sample, was used. Endosomes were solubilized with non-ionic detergent. Band intensities were quantified using the Odyssey NIR Imager analysis system as described[63], or the Quantity One program (Bio-Rad), for ECL detection. Radioactively labelled proteins were scanned using a Storm840 scanner (Amersham Biosciences) and band intensities were quantified using the ImageQuant software (Molecular Dynamics, Amersham).

Immunofluorescence microscopy, confocal microscopy and image analysis. Cells were grown on Transwell filters for indicated times, then fixed in 4% (v/v) paraformaldehyde and processed for immunofluorescence microscopy staining as previously described[21]. pIgA treatment was for 15 min. Confocal microscopy images, including stacks, were acquired using a Zeiss LSM510 confocal microscope, and image analysis was performed using accompanying software or Adobe Photoshop and Illustrator for image contrast. For co-localization quantification, Zeiss LSM510 software was utilized to either calculate Pearson's correlation coefficient (R^2), from images containing ≥ 50 cells, or for *x*–*z* reconstructions from confocal microscopy stacks.

pIgR secretory component delivery and pIgA transcytosis assays. These assays are as previously described[6,24]. Sheep anti-secretory-component antibodies cross-linked to protein G beads were used to immunoprecipitate ^{35}S-labelled pIgR and secretory components. Guinea pig anti-secretory component and mouse anti-biotin antibodies were used for immunoprecipitation and immunoblotting of biotinylated secretory components.

For general pIgA transcytosis assays, cells were treated with 100 μg ml^{-1} biotinylated pIgA at the basolateral surface at 37 °C for 15–60 min as indicated in Figures 4b, 5f and 6d. For pIgA transcytosis and pIgA subapical accumulation at 17 °C (Fig. 7b), cells were treated with biotinylated pIgA at the basolateral surface for 10 min at 37 °C, then washed at 17 °C for 30 min to accumulate pIgA intracellularly[21]. Apically released pIgA was measured after incubation at 37 °C for 30–60 min. The apical medium samples and the cell lysates were collected for ELISA analysis. Apically transcytosed pIgA was calculated as the percentage of total pIgA (apical pIgA plus intracellular pIgA).

ELISA (enzyme-linked immunosorbent assay) for pIgA transcytosis analysis. The amount of biotinylated pIgA, collected from either the apical medium after transcytosis or remaining in cells, was measured by ELISA. Briefly, Streptavidin-coated 96-well plates were blocked with 2% (w/v) BSA (bovine serum albumin) in PBS. Samples collected at different times, were diluted in 2% BSA in 0.5% (v/v) PBST (phosphate-buffered saline Tween 20) and pre-incubated at 37 °C for 1 h. Wells were first treated with mouse anti-biotin antibody (1:5000) for 2 h at 37 °C, and then with HRP-conjugated rabbit anti mouse IgG (1:10,000) for 1 h at 37 °C. TMB (3, 3′, 5, 5′-tetramentylbenzidine) substrate (kit from Pierce) was used for detection. Data was analysed by Softmax (Molecular Device). A similar ELISA was also performed to measure fluid-phase transcytosis of biotinylated HRP.

Statistics. Data are expressed as means ± s.e.m. Student's *t* test was used to compare differences between treated groups relative to their paired controls. *P* values are indicated in the text and figures above the two groups compared.

Transepithelial resistance (TER) measurements. TER was measured using an epithelial volt-ohm meter, Millicell-ERS (Millipore, Billerica, MA) for filter grown cells. The absolute TER values were determined according to manufacturer's instructions.

50. Polson, A. G. *et al.* Kaposi's sarcoma-associated herpesvirus K-bZIP protein is phosphorylated by cyclin-dependent kinases. *J. Virol.* **75,** 3175–3184 (2001).
51. Witucki, L. A. *et al.* Mutant tyrosine kinases with unnatural nucleotide specificity retain the structure and phospho-acceptor specificity of the wild-type enzyme. *Chem. Biol.* **9,** 25–33 (2002).
52. Bishop, A. C. *et al.* Generation of monospecific nanomolar tyrosine kinase inhibitors via a chemical genetic approach. *J. Am. Chem. Soc.* **121,** 627–631 (1999).
53. Duronio, R. J. *et al.* Protein *N*-myristoylation in *Escherichia coli*: reconstitution of a eukaryotic protein modification in bacteria. *Proc. Natl Acad. Sci. USA* **87,** 1506–1510 (1990).
54. Franco, M., Chardin, P., Chabre, M. & Paris, S. Myristoylation of ADP-ribosylation factor 1 facilitates nucleotide exchange at physiological Mg^{2+} levels. *J. Biol. Chem.* **270,** 1337–1341 (1995).
55. Sun, G. & Budde, R. J. Expression, purification, and initial characterization of human Yes protein tyrosine kinase from a bacterial expression system. *Arch. Biochem. Biophys.* **345,** 135–142 (1997).
56. Lindsay, A.J. & McCaffrey, M.W. The C2 domains of the class I Rab11 family of interacting proteins target recycling vesicles to the plasma membrane. *J. Cell Sci.* **117,** 4365-75 (2004).
57. Mostov, K. E., de Bruyn Kops, A. & Deitcher, D. L. Deletion of the cytoplasmic domain of the polymeric immunoglobulin receptor prevents basolateral localization and endocytosis. *Cell* **47,** 359–364 (1986).
58. Greulich, H. *et al.* Oncogenic transformation by inhibitor-sensitive and -resistant EGFR mutants. *PLoS Med.* **2,** e313 (2005).
59. Stegmeier, F., Hu, G., Rickles, R. J., Hannon, G. J. & Elledge, S. J. A lentiviral microRNA-based system for single-copy polymerase II-regulated RNA interference in mammalian cells. *Proc. Natl Acad. Sci. USA* **102,** 13212–13217 (2005).
60. Moffat, J. *et al.* A lentiviral RNAi library for human and mouse genes applied to an arrayed viral high-content screen. *Cell* **124,** 1283–1298 (2006).
61. Belcher, J. D. *et al.* Isolation and characterization of three endosomal fractions from the liver of estradiol-treated rats. *Proc. Natl Acad. Sci. USA* **84,** 6785–6789 (1987).
62. Ulrich, S. M., Kenski, D. M. & Shokat, K. M. Engineering a 'methionine clamp' into Src family kinases enhances specificity toward unnatural ATP analogues. *Biochemistry* **42,** 7915–7921 (2003).
63. O'Brien, L. E. *et al.* ERK and MMPs sequentially regulate distinct stages of epithelial tubule development. *Dev. Cell* **7,** 21–32 (2004).

nature cell biology

DOI: 10.1038/ncb2118

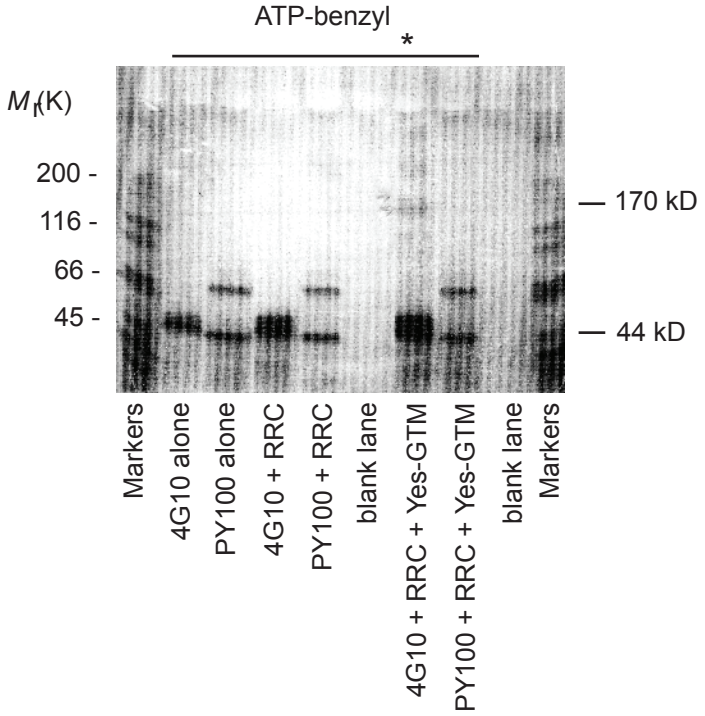

Figure S1 Identification of EGFR as a Yes substrate on rat liver endosomes by affinity purification and mass spectrometry. Tyrosine-phosphorylated proteins from rat liver endosomes were affinity purified by anti-phosphotyrosine (4G10, pY100) antibodies from a kinase reaction (t = 4 min; see methods). The 170 kD band (indicated with *) was identified as rat EGFR by mass spectrometry. Presented is a representative silver stained gel used for mass spectrometric analysis. Note, the 170 kD band could only be isolated using 4G10.

a

		pIgR-Yes	pIgR-EGFR	Yes-EGFR
control	sub-Ap	0.43	0.20	0.20
	middle	0.31	0.08	0.09
+pIgA	sub-Ap	0.00	0.00	0.02
	middle	0.12	0.09	0.11

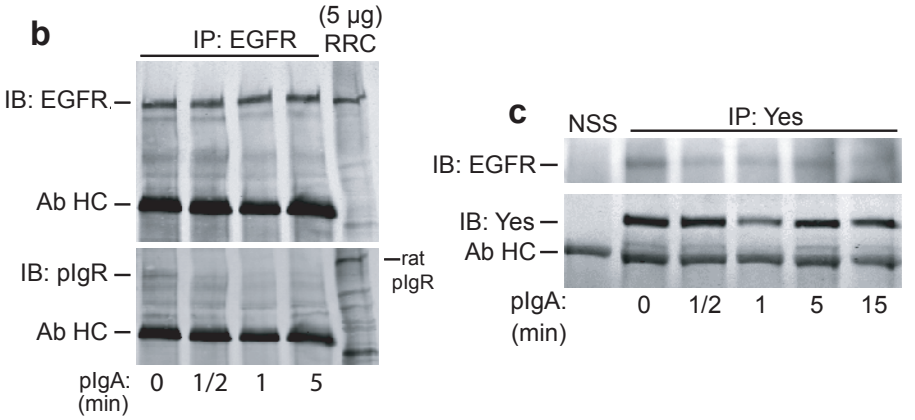

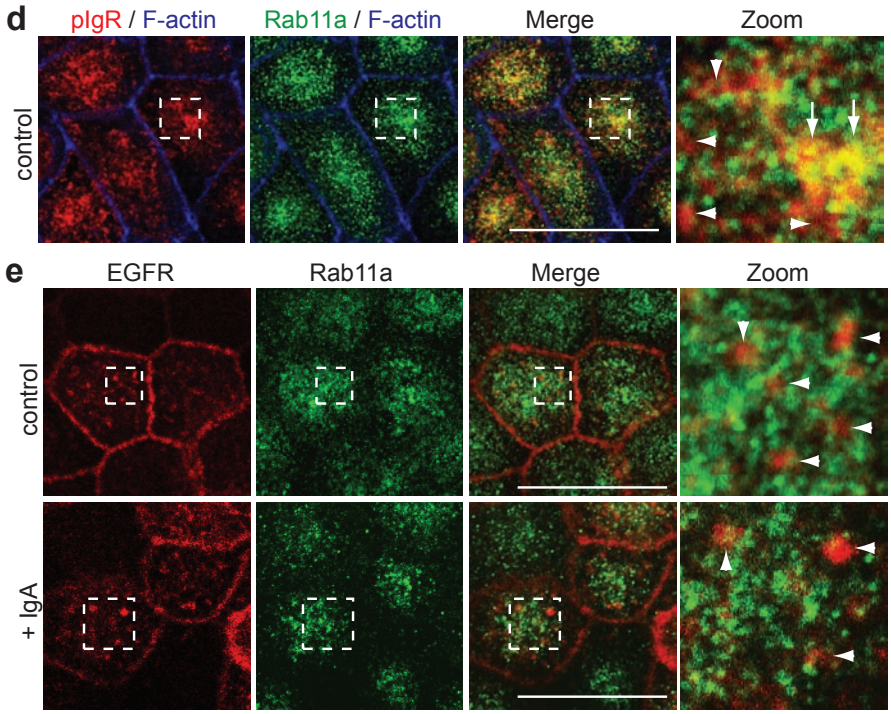

Figure S2 pIgR-Yes-EGFR complex interaction and localization. (**a**) Quantification of co-localization between pIgR, Yes, and EGFR from Figure 3c. Presented numbers in table (Pearson's correlation coefficient; R^2) represent co-localization index between indicated proteins, and under indicated conditions, performed using Zeiss LSM 510 confocal software. R^2 was calculated from images of monolayers of ≥ 50 cells. (**b,c**) pIgA stimulation reduces co-immunoprecipitation of pIgR-EGFR (**b**) and EGFR-Yes (**c**) complexes. MDCK-pIgR monolayers were treated with pIgA basolaterally for indicated times, then immunoprecipitated (IP) for EGFR (**b**) or Yes (**c**). Immunoprecipitates were blotted for the presence of EGFR and pIgR (**b**) or EGFR and Yes (**c**). 5 µg RRC fraction was used as a positive control (**b**), while non-specific sera (NSS) was used as a negative control for precipitations (**c**). Note, pIgR-EGFR co-IP with and EGFR-Yes co-IP were decreased after 30 seconds of pIgA stimulation. (**d**) A pool of pIgR co-localizes with Rab11a. Filter-grown monolayers of pIgR-MDCK were stained for pIgR (red), Rab11a (green) and F-actin (blue). Note overlap of a pool of pIgR with Rab11a (arrow) in the subapical region of cells, while other vesicles containing pIgR are devoid of Rab11a (arrowheads). (**e**) EGFR does not localize to a Rab11a compartment. Filter-grown monolayers of pIgR-MDCK stably expressing hEGFR were stained for EGFR (red) and Rab11a (green) without (control) or with pIgA stimulation (15 min). Note lack of overlap between vesicular EGFR (arrowheads) and Rab11a in the subapical region of cells. Zoom, magnified image of boxed region. Bar, 20 µm.

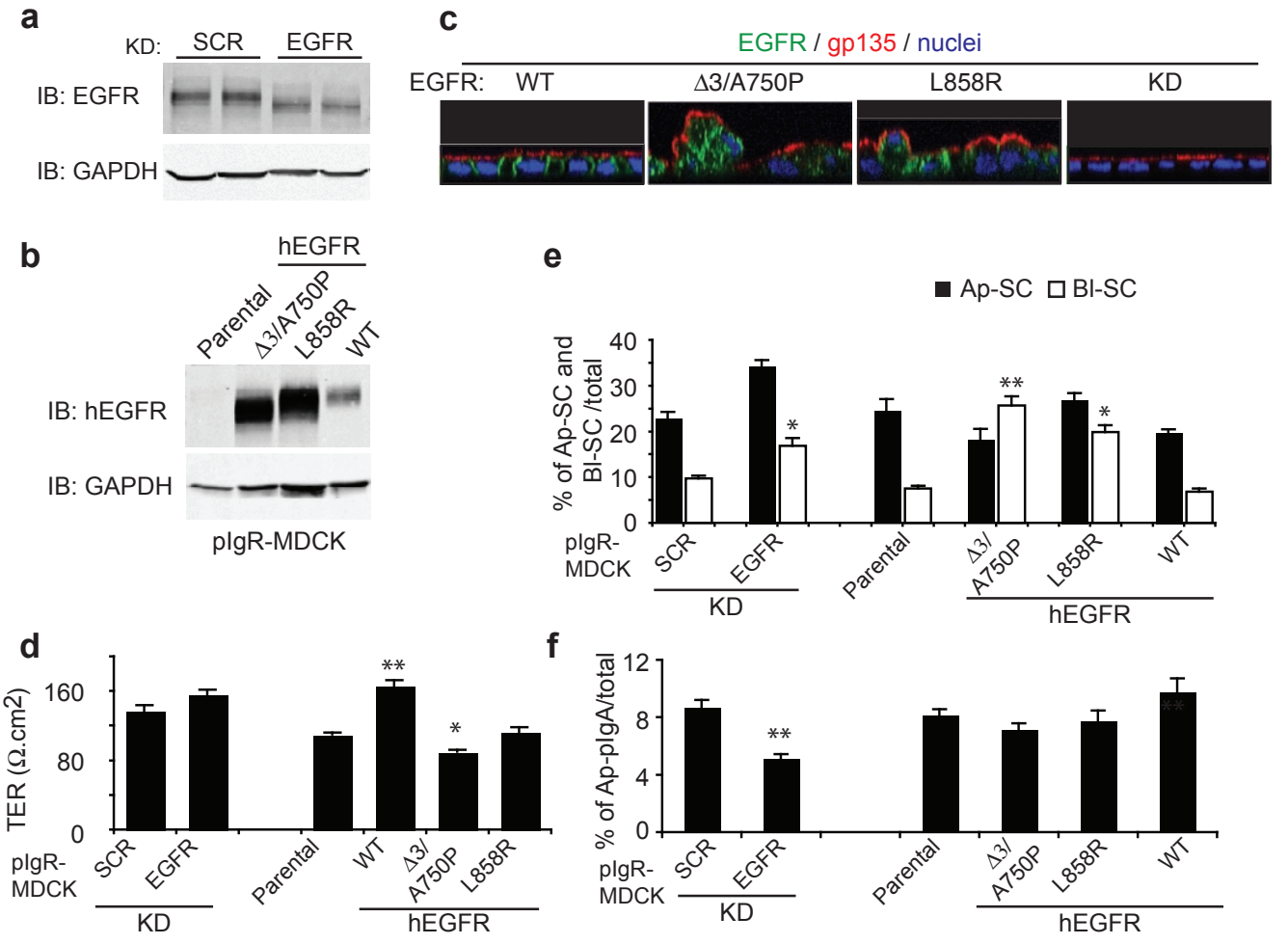

Figure S3 EGFR regulates pIgR and pIgA transcytosis. **(a)** Knockdown (KD) of EGFR in pIgR-MDCK cells. EGFR shRNA decreased EGFR expression by ~ 70%, compared to control scramble (SCR) shRNAs. WB is presented as duplicate KD samples, with GAPDH as a loading control. **(b)** Overexpression of hEGFR variants. pIgR-MDCK cells (parental) stably expressing two different constitutively active (Δ3/A750P, L858R) or WT hEGFR variants were blotted for hEGFR expression, or GAPDH as a control. Note, the anti-hEGFR antibody detects exogenous human, but not endogenous canine, EGFR. **(c)** Monolayer morphogenesis is disrupted by constitutive EGFR activation. Filter-grown (72 h) MDCK over expressing exogenous hEGFR alleles (WT, Δ3/A750P, L858R) or with endogenous EGFR KD were immunolabelled for gp135 (red), EGFR (green) and nuclei (blue). Note that constitutive (Δ3/A750P, L858R) but not WT EGFR activation causes bulging of cells out of the monolayer without disrupting apical gp135 polarization. Apical gp135 polarization is similarly maintained upon EGFR KD, though monolayers were slightly shorter than WT EGFR cells. **(d)** Transepithelial electrical resistance (TER) in EGFR-altered monolayers. TER ($\Omega.cm^2$) was measured in filter grown (48 h) monolayers of parental pIgR-MDCK, or monolayers expressing shRNA (SCR, EGFR KD) or hEGFR alleles (WT, Δ3/A750P, L858R). Note increase in TER upon (WT) overexpression, and slightly decreased TER upon Δ3/A750P EGFR overexpression. Asterisk indicates $P< 0.05$, double asterisks indicate $P < 0.001$; all data are mean ± s.e.m.; n = 4. **(e)** SC release is affected by EGFR expression. Filter-grown (72 h) pIgR-MDCK monolayers were biotinylated at the basolateral surface at 17ºC, then transferred at 37ºC for 60 min of transcytosis. The biotinylated SC released into the apical and basolateral media and biotinylated pIgR in cell lysates were measured by IP and immunobloting (see Methods). In CA-EGFR cells (Δ3/A750P, L858R) Bl-SC release was significantly increased compared to parental cells (Δ3/A750P [25.7%] and L858R [19.8%] vs parental 7.5%, $p<0.01$, n=3). Note, EGFR KD resulted in non-polarized release of SC, in both apical and basolateral directions. **(f)** EGFR promotes apical pIgA transcytosis. Apical transcytosis of pIgA was significantly decreased upon EGFR KD (6.5 ± 0.36 %) compared to SCR cells (10.9 ± 0.61%) after 30 min of transcytosis (mean ± s.e.m., n=8, $P< 0.001$). In contrast, indicated EGFR alleles failed to influence apical transcytosis of pIgA.

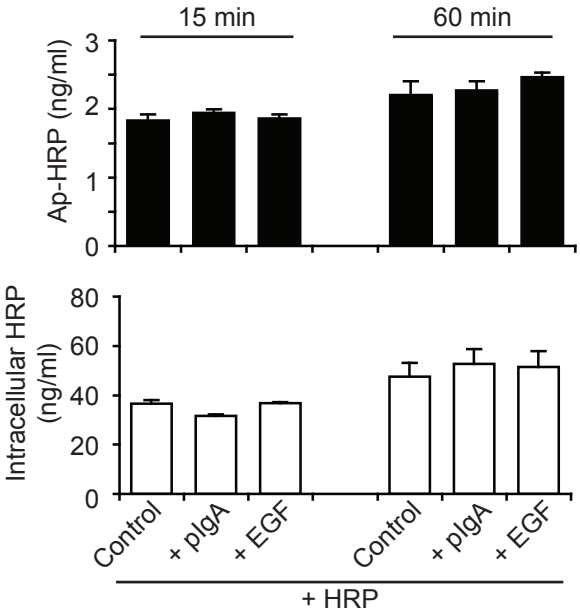

Figure S4 Examination of HRP transcytosis. HRP transcytosis is not affected by pIgA or EGF treatment in pIgR-MDCK cells. Monolayers were incubated basolaterally with biotinylated HRP (0.2 mg/ml) alone, or in combination with pIgA (0.3 mg/ml) or EGF (100 ng/ml). Apical medium and cell lysates were collected at 15 or 60 min. Transcytosed and intracellular HRP were measured by ELISA (see Methods). No significant difference in HRP trafficking was observed upon pIgA or EGF stimulation (mean ± s.e.m., n=3).

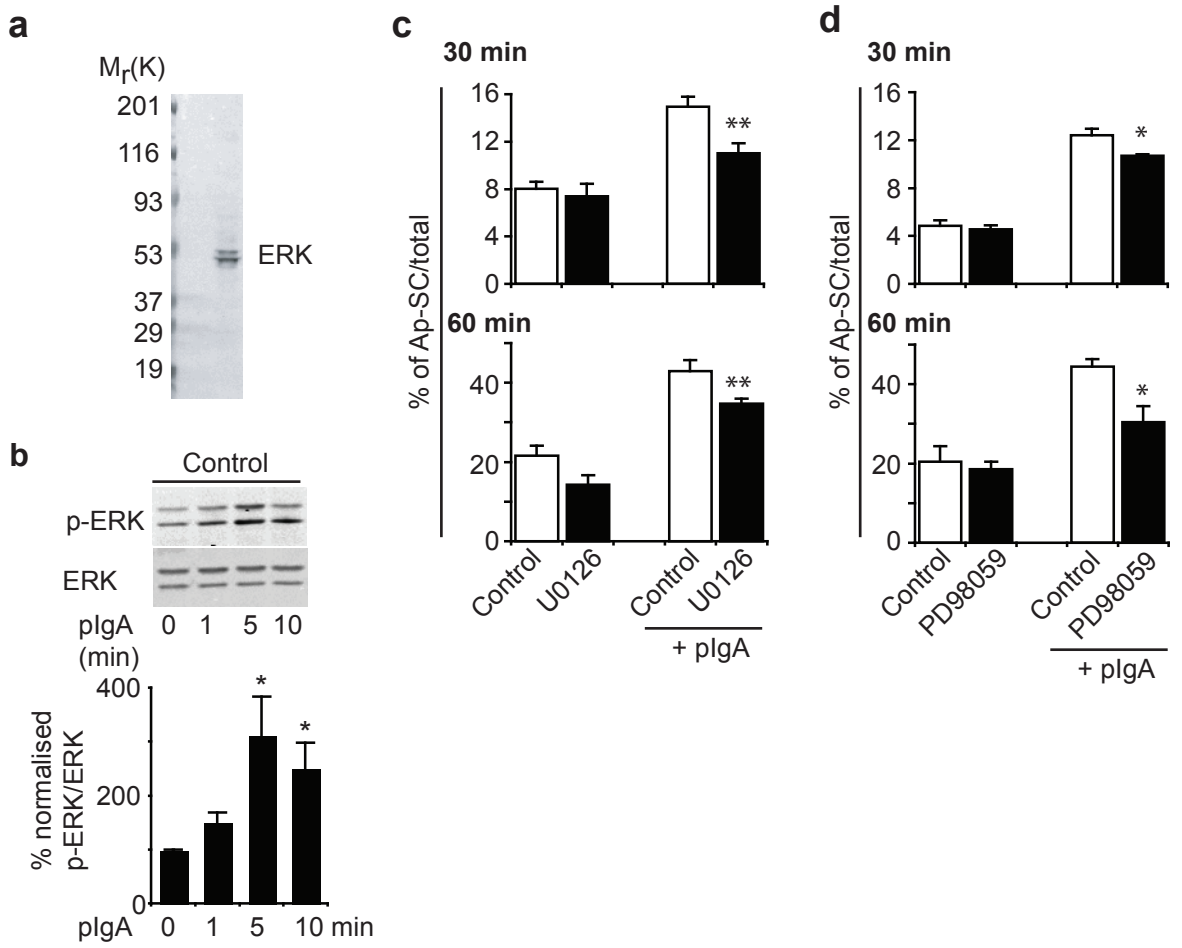

Figure S5 ERK is present on RRC and involved in pIgA-pIgR transcytosis. (**a**) Blotting of RRC fractions revealed that ERK1/2 are present on rat liver endosomes in vivo. (**b**) EGFR-pIgR-MDCK cells were treated basolaterally with pIgA for indicated times. Cell lysates (20 µg protein/lane) were analyzed by immunoblotting with specific pERK and total ERK antibodies. Quantitation (below each blot) shows a peak of pERK/ERK increase at 5 min of 210 ± 0.68 % over controls (mean ± s.e.m., n=3, $P < 0.03$). **(c, d)** Inhibition of MEK activity decreases pIgA-stimulated SC-apical release in pIgR MDCK cells. MDCK monolayers were metabolically labelled with ^{35}S-cysteine and basolaterally treated with pIgA as described in Fig. 4, with or without inhibitors (10 µM U0126 or 50 µM PD98059). Apical and basal medium, and cell lysates were collected at indicated points and immunoprecipitated for pIgR. Apically released SC (Ap-SC) is presented as a percentage of total labelled pIgR. Each group includes 6-8 samples from 3-4 separate experiments. Note, pIgA-stimulated Ap-SC release was inhibited by the MEK inhibitors U0126 **(b)** or PD98059 **(c)** both at 30 and 60 min. Asterisk indicates $P < 0.05$, double asterisks indicate $P < 0.001$; all data are mean ± s.e.m., n = 6.

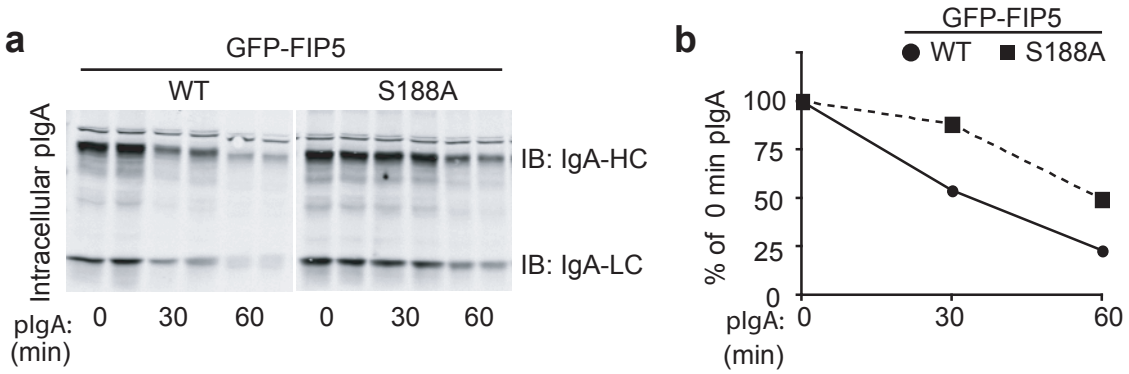

Figure S6 FIP5 S188A results in intracellular retention of pIgA. (**a**) S188A mutation increases pIgA intracellular retention. Cells were basolaterally treated with biotinylated pIgA for 10 min, then washed at 17°C for 30 min and incubated at 37°C to induce transcytosis. Lysates were blotted for pIgA remaining intracellularly (pIgA heavy chain, HC and light chain, LC as indicated, a non-specific band above HC treated as a loading control). (**b**) Quantification of pIgA levels from (**a**), representative of the percentage of pIgA remaining intracellularly (compared to 0 min) for WT or S188A GFP-FIP5-expressing cells (average of band densities).

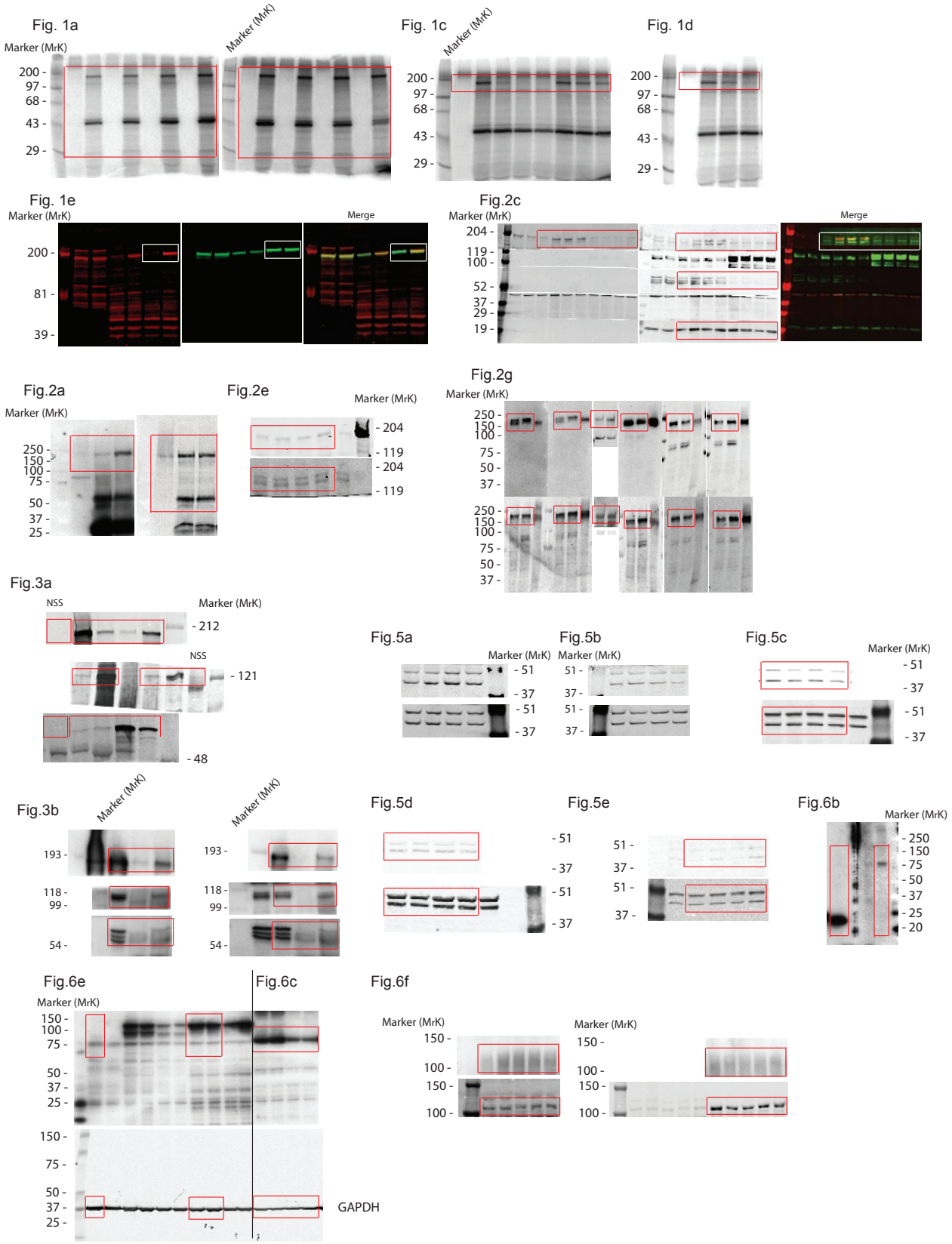

Figure S7 Full scans of western blots from main figures.